A METHOD TO PREDICT THE MODIFICATION OF SEA STATE BY CURRENTS AT CAPE MUDGE AND SAND HEADS IN THE STRAIT OF GEORGIA

Prepared for the
Institute of Ocean Sciences
Department of Fisheries and Oceans
Patricia Bay, B.C.

by

PACIFIC OCEAN SCIENCES LTD.
Burnaby, B.C.

August, 1987

Table of Contents

1 INTRODUCTION 3

2 THEORY 4
2.1 BACKGROUND 4
2.2 THE SMB METHOD 5
2.3 WAVE-CURRENT INTERACTION 8

3 APPLICATION TO THE STRAIT OF GEORGIA 11
3.1 CAPE MUDGE 11
3.2 SAND HEADS 14

4 DISCUSSION AND RECOMMENDATIONS 16
4.1 COMPARISON OF AVAILABLE APPROACHES 17
4.1.1 CHARACTERISTIC MODELS 18
4.1.2 PARAMETRIC HYBRID MODELS 19
4.1.3 DISCRETE SPECTRAL MODELS 21
4.1.4 SUMMARY OF APPROACHES 22

5 REFERENCES 23

6 TABLES 25

7 FIGURES 27

List of Figures

Figure 1. Plan view of the Strait of Georgia indicating the estimated fetch at Cape Mudge for SE winds (90 km) and at Sand Heads for SW winds (22km).

Figure 2A. The geometry of a plane wave illustrating wave height H, wave length L, and mean wave slope α .

Figure 2B. A schematic illustration of the importance of wave slope.

Figure 3. Wave steepness δ as a function of wave age β (from Kinsman, 1965).

Figure 4. A schematic illustration of the ray backtracing proceedure for a location in Queen Charlotte Sound (from Stronach and Helbig, 1986).

Figure 5. The modification of a wave spectrum by wave-current interaction. The solid line represents the incident spectrum (H_s = 1.4 m); the line of short dashes represents the spectrum when waves propagate with a following current of 1 m/s (H_s = 1.21 m), and the line of longer dashes represents the spectrum when waves propagate into an opposing current of 1 m/s (H_s =1.73 m).

Figure 6. Time series of height enhancement factors for Cape Mudge. The first 72 hours ofJune 1987 are shown, for waves of peak period 4 s (long dashes) and 8 s (short dashes). The tidal current time series is also plotted.

Figure 7A. Forecasting chart 1 for Cape Mudge.

Figure 7B. Forecasting chart 2 for Cape Mudge. Wave heights (solid lines) are given in metres; wave periods (dashed lines) are given in seconds. The area to the right of the heavy solid line represents a fully developed sea.

Figure 8. Hypothetical Cape Mudge windfield for June 1, 1987 and SMB predicted wave height and period.

Figure 9. The range of relevant ray directions for Cape Mudge.

Figure 10. Significant wave height and wave slope enhancement factors for June 1, 1987. Time is in PST. Also listed are the up-strait (v) and cross-strait (u) components of the tidal current in m/s and the tidal elevation (z) at Cape Mudge.

Figure 11. Significant wave height enhancement factors at Cape Mudge for June 1, 1987: (1) vs. time for 2 second waves (*); (2) vs. wave period at 0400 hours (+, lower curve); (3) vs. wave period at 1700 hours (+, upper curve).

Figure 12. The grid system for the Crean tidal models (from Crean, 1983)

Figure 13. The JONSWAP frequency spectrum.

List of Tables

Table 1. SMB Constants

Table 2. Hypothetical SMB Forecast for Cape Mudge, June 1, 1987.

Preface

This work was carried out under contract DSS FP941-6-1942 for the Institute of Ocean Sciences under the direction of Dr. J.F. Garrett by Drs. J.A. Helbig and J.A. Stronach of Pacific Ocean Sciences Ltd. We are very pleased to acknowledge Dr. Garrett's support.

EXECUTIVE SUMMARY

A simple wave prediction model was coupled to a wave-current interaction model to predict the enhancement or damping of wave height and wave slope at Cape Mudge and Sand Heads in the Strait of Georgia (Figure 1). The Sverdrup - Munk - Bretschneider (SMB) model was used to predict significant wave height and period at these two locations. A scheme developed by Stronach and Helbig (1986) to estimate wave-current effects was used to adjust the SMB predictions. In addition a measure of enhanced wave slope was provided. A set of tables listing the enhancement factors was published for the period April 1987 - March 1988 and is attached.

Currents at Cape Mudge and Sand Heads were obtained from the 2 km mesh barotropic tidal model of Crean (1983). At Sand Heads, these tidal currents were augmented with a Fraser River induced flow estimated from measured data and assumed to depend heavily on the Fraser River discharge. The Fraser River discharge for 1978 was used because 1978 was similar to 1987 in terms of snowpack.

This report describes an initial effort at describing the effects of wave-current interaction in the Strait of Georgia. During the preparation of the report, a number of shortcomings and potential improvements were noted. Consequently, we offer the following recommendations:

- First, and of foremost importance, simultaneous wave and current measurements must be obtained at these two locations - the model must be calibrated as well as validated. Until it is, the results obtained here are only estimates, albeit conservative ones. Moreover, the available current data from Sand Heads are of low quality.

- Second, near real time Fraser River discharge must be used, since long term forecasts are of low accuracy. Consequently, the full procedure should be automated to run on a computer and should prompt the user for both winds and discharge, thus eliminating the need for charts and published enhancement factors.

- Third, the model should be extended to the full Strait of Georgia - Juan de Fuca system since wave-current effects are not truly limited to Cape Mudge or Sand Heads. Moreover, even if we are interested solely in these locales, spatially varying currents must play some role in modifying the waves along the fetch, especially at Cape Mudge.

- Fourth, the SMB technique should be replaced with a more accurate one capable of predicting the directional spectrum. Several general options are discussed fully in the report. In any case, the model selected must serve the dual purpose of providing wave forecasts for the full system as well as predicting wave-current effects. The wave model should meet the following minimum set of requirements:

(1) It should be compatible with either the GF7 (2 km grid) or GF4 (4 km grid) tidal models of Crean (1983);

(2) At the very least, it should predict peak period, direction, and some indication of peak shape and directional spread;

(3) It should be readily amended to include wave-current effects.

(4) It should run on a system no larger than an IBM-AT or equivalent, and it must be extremely user-friendly.

(5) It should include non-linear wave-wave interaction.

(6) If the model is extended to Juan de Fuca Strait, it should be capable of propagating open ocean swell into the system.

It is not necessary at this stage to: (1) include shallow water effects (enhanced non-linear interaction and dissipation), or (2) treat the tidal passes connecting Fuca and Georgia (Haro Strait, Boundary Pass), except in a straightforward manner, because the fetch in such regions is very limited. However, the model selected should be adaptable to shallow water to permit future modifications. For the reasons given in Section 4, we recommend the adoption of a parametric model based on the JONSWAP spectrum.

1 INTRODUCTION

Two regions in the Strait of Georgia, Cape Mudge and Sand Heads (Figure 1), are known for having unusually rough and choppy seas during certain stages of the tide and for certain winds (Dept. of Fisheries and Oceans, 1979). Specifically, the Coast Pilot warns that the area between Cape Mudge and Vancouver Island is subject to short steep waves that can be very dangerous to small vessels when a southeastward current is opposed by a strong southeast wind. (Note that the meteorologist's convention is being used for winds and the oceanographer's convention is used for currents: Winds are referenced by the direction from which they blow and currents by the direction to which they flow.) Similarly, off Sand Heads in the mouth of the Fraser River, the Pilot warns of rough seas that have swamped numerous small craft when a southwest wind blows against currents induced by the Fraser River freshet.

Both cases are classic examples of wave-current interaction (Longuet-Higgins and Stewart, 1964) in which a wave train extracts energy from the surface flow and increases in height when it runs into an opposing current. In effect, the waves are forced to "stand up" by the flow. Conversely, when waves advance into a region in which the current increases along the wave direction, the flow will extract energy from the waves, the wave height will decrease, and the sea will become calmer. In other words, the waves are "stretched out" by the currents. Needless to say, the Pilot does not comment on this latter effect. The closer the direction of the surface flow (parallel or anti-parallel) is to the wave propagation direction, the more intense is the interaction.

Since wave speed decreases with increasing frequency, it is the relatively high frequency (i.e. small period) waves that are most strongly affected. A subtle consequence of this is that mean wave slope is more sensitive than wave height to wave-current interaction. Thus opposing currents not only amplify wave height, they also generate more peaked seas. Indeed it is often the wave slope that is of greatest concern to boaters (Figure 2B).

This report describes a simple and straightforward technique for estimating the effects of wave current interaction at Cape Mudge and Sand Heads in the Strait of Georgia. Briefly, the SMB method is used to predict significant wave height and wave period given a history of winds, and then conservation of wave action is invoked to estimate current and shoaling effects. This is done by using a ray backtracking procedure developed by Stronach and Helbig (1986) for application in the waters surrounding the Queen Charlotte Islands.

The structure of this report is as follows. A very brief account of the necessary theory is given in Section 2, while application to the Strait of Georgia is made in Section 3 together with the presentation of some sample results. A critique of the method follows (Section 4), and a series of recommendations and alternatives for both improving wave forecasts in the Juan de Fuca - Strait of Georgia system as well as incorporating wave current effects is made. A manual describing the everyday application of the method is attached as are hourly listings of wave height and wave slope enhancement factors for the period April 1987-March 1988. A set of floppy discs containing these listings is also appended.

2 THEORY

2.1 BACKGROUND

Prior to describing the SMB method and wave-current interaction, a few preliminary results are quoted for the non-oceanographer. The starting point for all wave theory is the simple plane wave (Figure 2) in which the sea surface elevation η at any point $\underline{x}=(x,y)$ is given by

$$\eta = (H/2)\cos(\omega t - \underline{k}\cdot\underline{x}) \tag{1}$$

Here H is the wave height, ω is the radian frequency which is related to the circular frequency f and the wave period T by

$$\omega = 2\pi f = 2\pi/T \tag{2}$$

and $\underline{k} = k(\cos\theta, \sin\theta)$ is the wavenumber which points in the direction of wave propagation θ with magnitude k, and is in turn related to the wavelength L

$$k = 2\pi/L. \tag{3}$$

The frequency and wavenumber of each packet are linked through the dispersion relation

$$\omega^2 = gk\tanh(kh) \tag{4}$$

where g is the acceleration due to gravity and h is the water depth. Note that as the wavelength decreases, the frequency increases: short waves have small periods and long waves have large periods. Thus it follows that for a given wave height, short waves are much steeper than long waves (Figure 2).

The plane wave is an idealized concept, and the real sea state is best thought of as being composed of a sum of a large number of "wave packets", each a bundle of nearly plane waves centred on its own frequency and direction. The total energy m_o of the wavefield is thus a sum over the energy of the individual packets

$$m_o = \int\int E(\omega,\theta)\,d\omega\,d\theta \tag{5}$$

where the directional wave spectrum $E(\omega,\theta)$ is the energy density of the wave packet in (ω,θ) space. The goal of modern wave theory is to predict $E(\omega,\theta)$ given the overlying windfield. For many purposes including the present one, knowledge of the full wave spectrum is not necessary, and an adequate wave forecast can be obtained in a less complicated manner, as is described later.

For example, the sea state is commonly characterized by its "significant wave height" H_s and "significant wave period" T_s. H_s is related to $E(\omega,\theta)$ through

$$H_s = 4\cdot m_o^{1/2} \tag{6}$$

(ignoring constant factors required for dimensional fidelity) and is roughly the wave height that an experienced observer would report from a visual sighting. More precisely, it is (almost) the average of the highest one third of waves in a wave field. It is important to understand that H_s is not the height of the largest wave expected; rather it is an average value weighted towards the larger waves present. (The reader is referred to LeBlond (1981) for a more extensive discussion of the distribution of wave heights and periods and individual extreme waves.) T_s is the corresponding period. Frankly, in practice its definition is often fuzzy, and we choose T_s as the period corresponding to the peak of the spectral density.

While the significant wave height gives a good measure of roughness, it does not indicate wave slope, that is the "choppiness" of the sea. The slope of an individual plane wave is given approximately by the ratio of wave height to wave length (Figure 2). For the sea state as a whole, the mean slope is defined as the average over the individual wave slopes

$$S_m = \left\{ \int k^2 E(\omega,\theta) d\omega d\theta \right\}^{1/2} \tag{7}$$

Since wave-current interaction is a frequency dependent phenomenon and short waves generally interact more strongly than do longer waves, it follows that slope is more sensitive to currents than wave height. Thus an adverse current can make the sea very choppy and dangerous to small craft, even though wave height is relatively small. The mean slope is rarely specified or issued with wave forecasts; it is included here for interest and to generate comment on its utility as a measure of the sea surface.

2.2 THE SMB METHOD

The Sverdrup-Munk-Bretschnider (SMB) method for predicting significant wave height and period was developed during World War II (Sverdrup and Munk 1947) and subsequently modified by Bretschnider (1952). It was developed prior to a thorough understanding of wave dynamics and prior to the availability of estimates of $E(\omega,\theta)$, and it suffers as a consequence, as is discussed in Section 4. On the other hand, it is largely based on the fitting of curves to observed data and thus partially transcends its theoretical limitations. Indeed, it has been applied throughout the world with considerable success and continues to be used in many coastal engineering applications. It has the advantage of being quick and easy to apply, and probably errs on the side of conservatism; that is it somewhat overestimates the sea state. The original formulation is cast partly in terms of the significant wave, *i.e.* that fictitious wave with period T_s and wave height H_s. By contrast, the account presented here is much more modern and consequently tends to highlight the weakest points of the old theory. This is no doubt unfair, but unavoidable. A general discussion is contained in Kinsman (1965); its practical application is discussed by US Army Corps of Engineers (1975).

The SMB method, as a predictor of H_s, must ultimately be based on the balance equation for wave energy

$$\partial m_o / \partial t + c_g \partial m_o / \partial x + m_o \partial c_g / \partial x = S \tag{8}$$

Here the coordinate system is chosen such that x points in the direction of wave propagation; c_g is the mean group speed averaged over direction and frequency of the wave field and is the speed at which wave energy propagates. The source term S includes both forcing by the wind as well as a number of dissipative processes; its precise form is not important here. Equation (8) forms the basis for several operational wave prediction models including the NOWAMO and the KNMI models (Guddal, 1985; and deVoogt, *et al.*, 1985).

The SMB method is based on simplified versions of (8) that follow from two general observations for idealized situations, namely those in which the winds are turned on at some arbitrary time and are horizontally homogeneous over the region of interest. (The more general case of a time varying wind is considered later.) In Case 1, which applies to initial stages of wave growth, wave height and period are limited solely by duration, *i.e.*, that length of time the wind blows. Over the region covered by the wind, H_s and T_s grow uniformly until the minimum duration time t_D is reached. For longer times the wavefield is no longer horizontally uniform but rather depends on the fetch F, i.e. the distance over which the wind blows. In the second case of fetch limited growth, H_s and T_s are time independent but increase with fetch. In practice the fetch is limited either by a coastline or to the less well defined distance over which the wind is nearly unidirectional, that is the distance on a surface pressure map over which the curvature of isobars can be ignored. For a given fetch, the minimum duration is defined as the time it takes a "significant" wave to travel across the fetch, namely $t_D=F/c_g$.

Mathematically, the duration limited case is defined by assuming that wave energy and wave period are spatially independent. However, they remain time dependent and this is expressed in (8) by replacing $\partial c_g/\partial x$ with $c_g^{-1}\partial c_g/\partial x$, to obtain

$$\partial m_o/\partial t + m_o c_g^{-1}\partial c_g/\partial t = S \tag{9}$$

Similarly, in the fetch limited case, all time dependence is ignored and (8) becomes

$$c_g\partial m_o/\partial x + m_o\partial c_g/\partial x = S \tag{10}$$

Ultimately, the sea becomes "fully developed" as the significant wave height and period attain constant maximum values consistent with the fetch F. Dissipation through wave breaking and other mechanisms exactly balances wind input, S vanishes, and wave growth ceases.

Note that both (9) and (10) may be rewritten in terms of wave energy flux

$$\begin{pmatrix} c_g^{-1}\partial/\partial t \\ \partial/\partial x \end{pmatrix} \cdot c_g m_o = S$$

With the identification $\partial/\partial t = c_g\partial/\partial x$, the two equations collapse to one.

Now (9) and (10) are single equations in two unknowns m_o and c_g. Hence the system is

underdetermined and more information must be provided if it is to be solved. Sverdrup and Munk overcame this problem by assuming that the left hand sides of (9) and (10) were separable. That is, taking (9) as an example, they arbitrarily set

$$\partial m_o / \partial t = (1 - r) S \tag{11}$$

and

$$c_g^{-1} m_o \partial c_g / \partial t = r S \tag{12}$$

in terms of a constant r to be determined empirically from observations. Actually, Sverdrup and Munk did not use m_o and c_g as independent variables, rather they used the non-dimensional quantities

$$\beta = c_g / 2W = c_p / W \tag{13}$$

and

$$\delta = H_s k / 2 = 2 k m_o^{1/2} \tag{14}$$

where W is the wind speed. β is known as the wave age; for $\beta < 1$, the wind works actively on the waves which increase in height and period. For $\beta > 1$, wind and waves are largely decoupled. c_p is the wave phase speed and in deep water is twice the group speed; it is the speed at which an individual wave crest travels. The parameter δ is a measure of waveslope (it is the ratio of H_s to the wavelength), and theoretically must be less than 1/7.

To solve (11)-(12) Sverdrup and Munk invoked a semi-empirical relationship between β and δ (Figure 3) and a form for S based on the theory of the day. Their solution (as later modified by Bretschnider, 1952) is of the form

$$H_s = a_1 \tanh\left(a_2 F^{*a_3}\right) \tag{15}$$

$$T_s = a_4 \tanh\left(a_5 F^{*a_6}\right) \tag{16}$$

$$t_D = a_7 \exp\left[a_8 (\ln F^*)^2 - a_9 \ln F^* + a_{10}\right] + a_{11} \ln F^* \tag{17}$$

Here F^* is the non-dimensional fetch

$$F^* = gF / W^2 \tag{18}$$

The constants a_i are listed in Table 1.

Given a constant windspeed W and a measured fetch F_0, (15)-(17) are applied as follows. First, the minimum duration is calculated from (17) using $F = F_0$. In the initial stages of wave growth, for which $t < t_D$, the effective fetch F_{eff} is computed by replacing t_D with t in (17), and inverting for F^*; clearly, $F_{eff} = F^*$ will be less than F_0. This value is then used in (15)

and (16) to find H_s and T_s. Later when t exceeds t_D, F assumes its limiting value F_0 and the wavefield is time independent. Thus for a given fetch there exist maximum values of H_s and T_s defining the fully developed state. However, real winds are not steady but vary with time. The SMB method is extended to this case by assuming the wind to be piecewise constant. The procedure is best illustrated by example and this is done in Section 3.2.

2.3 WAVE-CURRENT INTERACTION

Waves and currents can interact to exchange energy in the presence of spatially inhomogeneous surface currents: wave energy is not a conservative property and (8) no longer holds. In fact, it is no longer adequate to work in terms of m_o as the interaction is frequency dependent. Higher frequency waves, whose speeds are closest to current speeds, are most strongly affected. The spectral density $E(\omega,\theta)$ or, more correctly, the wave action density $E(\omega,\theta)/\omega_o$, becomes the proper variable. Here the intrinsic frequency ω_o is the frequency that a wave packet would have in the absence of currents. In terms of the observed frequency ω, it is given by

$$\omega_o = \omega - \underline{k} \cdot \underline{U} \tag{19}$$

Alternatively, ω_o follows directly from the dispersion relation (4) if k is known, as it often is in practice.

The theory at this stage is slightly complicated by a matter of convention. Strictly speaking it should be presented in terms of the energy density in $\underline{k}$ space $E(k_1,k_2)$ which satisfies

$$m_o = \int\int E(\underline{k})\,dk_1\,dk_2 \tag{20}$$

Then, in the absence of external forcing, wave action obeys

$$d\left[E(\underline{k})/\omega_o\right]/dt = 0 \tag{21}$$

along paths defined by

$$d\underline{x}/dt = \underline{c}_g + \underline{U} \tag{22}$$

$$d\underline{k}/dt = \nabla\cdot\left(\omega_o + \underline{k}\cdot\underline{U}\right) \tag{23}$$

The observed frequency along a ray satisfies

$$d\omega/dt = \underline{k}\cdot\partial\underline{U}/\partial t. \tag{24}$$

In practice ω is often nearly constant along the raypath, because a wave packet traverses the region of interest in a time short compared with the time scale of variation of $\underline{U}$. This is the

case in the present application.

Equation (21) may be rewritten in a highly informative manner for the energy density alone

$$dE(\underline{k})/dt = \left[E(\underline{k})/\omega_o\right] d\omega/dt = R_{ij}\partial U_i/\partial x_j \tag{25}$$

where the quantity R_{ij} is the radiation stress tensor. The importance of (25) is that it unequivocally illustrates that the flow must be sheared for waves and currents to exchange energy. If $\partial U_i/\partial x_j = 0$, i,j = 1,2, then the current advects the waves and shifts the observed frequency from its intrinsic value but does not exchange energy with it.

In terms of $E(\omega,\theta)$, (21) is

$$d\left[\left(2\pi k/c_g\omega_o\right)E(\omega,\theta)\right]/dt = 0 \tag{26}$$

However, in practice, conservation of wave action is exploited in polar (k,θ) space for which:

$$d\left[\left(k/\omega_o\right)E(k,\theta)\right]/dt = 0 \tag{27}$$

and the results are translated into (ω,θ) space. The bookkeeping is a bit messy but it is just that -bookkeeping- and depends solely on the way the different spectral densities have historically been scaled; in each case $m_o = \int E$. The physical content is exactly the same in each case.

The implication of action conservation is immediate: if E/ω_o is known at some point along the ray, it is known at all points. At any point $\underline{x}$, $E(k,\theta)$ can be constructed by "backtracking" the rays corresponding to fixed values of k and θ. That is the ray appropriate to a chosen value of k and θ and incident at $\underline{x}$ is followed backwards until it either strikes a coastline or a selected open boundary along which E and ω_o are known (Figure 4). In the former case, $E(k,\theta)=0$, and no contribution is made to wave energy at $\underline{x}$. Actually, a source term should be added to (27) to account for dissipation and wind input, but in the present application they can be ignored because only very short paths are of interest. It should be noted that refractive and shoaling effects generated by varying bathymetry are automatically included in this procedure through (22) and (23).

The open boundary case is especially easy to handle if the boundary transects a region of negligible currents, because then the intrinsic frequency equals the observed frequency. Thus for the case in which observed frequency is essentially constant, the intrinsic frequency follows directly from (19) if the current and wave direction are known. Otherwise, it must be computed from (24).

Of course, $E(k,\theta)$ is unknown and is not provided by the SMB method. In this application, we assume that it is adequately approximated by the extended Pierson-Moskowitz spectrum for a fully developed sea

$$E(\omega,\theta)=\alpha g^2\omega_m^{-5}\exp\left\{-(5/4)(\omega/\omega_m)^{-4}\right\}D(\theta) \tag{28}$$

which is defined in terms of the Phillips parameter α and the peak frequency ω_m. For the directional part $D(\theta)$, we use

$$D(\theta)=\begin{cases}(2/\pi)\cos^2(\theta-\phi) & |\theta-\phi|\le\pi/2\\ 0 & |\theta-\phi|\ge\pi/2\end{cases} \tag{29}$$

symmetric about the mean wave direction ϕ, which is assumed to be coincident with the wind. The cosine squared model is a very popular choice, and is warranted here since a more representative form for $D(\theta)$ has not yet been established. The total energy is given by

$$m_o=\int\int E(\omega,\theta)d\omega\,d\theta \tag{30}$$

or in terms of the significant height by

$$H_s=(16/5)^{1/2}\alpha g/\omega_m^2 \tag{31}$$

Thus the incident spectrum is fully defined in terms of prescribed values of H_s, T_s, and the wind direction ϕ.

With this formulation for the incident spectrum, the modified spectrum at the observation site is calculated by means of equations (19) and (27). For each element in (k,θ) space of the predicted spectrum, a hypothetical straight ray is projected back to the deeper waters where currents are assumed negligible. The modification in ω_o is calculated, based on the predicted tidal streams and the dispersion relation. This step is done iteratively because the dispersion relation is transcendental. It is then a trivial matter to identify the resulting modified incident spectral energy density with the required element of the predicted spectrum. Figure 5 illustrates the effect of current modification on a spectrum.

An incident spectrum correspondng to a peak period of 6 seconds and significant wave height of 1.4 m is assumed. (Note that when plotted against frequency, the spectrum peaks closer to 5 s, not 6 s. This is due to the choice of metric in frequency, since, we require that $m_o = \int E(\omega)d\omega = \int E(T)dT$, whereas $d\omega = (2\pi/T^2)dT$). In the presence of a following current of 1 m/s, the significant wave height is reduced to 1.21 m, while in the presence of an opposing current, the wave height grows to 1.73 m, correspondng to a 14% decrease and a 24% increase respectively.

When this calculation is repeated over several tidal cycles, the time series plotted in Figure 6 emerges. The tidal currents are for Cape Mudge, and in fact the data is taken from the tabulated wave enhancement factors to be discussed in Section 3. As expected, the wave enhancement factor is tidally modulated, and of opposite phase to the currents. In fact, this figure suggests that the wave enhancement factor would be ammenable to harmonic analysis and reconstruction, which could replace the labourious solution of transcendental equations and

spectral reconstruction mentioned in the above paragraph. It is noteworthy that the height enhancement factor responds more to opposing currents than to following currents - the relative maxima (values greater than 1.0) are considerably stronger than the relative minima (values less than 1.0).

Finally, The alternative formulation of Gonzales (1982) merits comparison with the present approach. Based on a comparative study of waves measured offshore and inshore of the Columbia River bar, Gonzales devised a scheme to predict the inshore energy spectrum E_{in} given the *measured* offshore spectrum $E_{off.}$ As we did here, he invoked the conservation of wave action but under the assumptions of: (1) time independence and (2) no cross channel flow. This allowed him to estimate a transfer function $T(\omega,\theta,,\underline{U})$ such that

$$E_{\epsilon}(\omega,\theta) = T(\omega,\theta,\underline{U}) \cdot E_{off}(\omega,\theta).$$

Here U is the Columbia River outflow modulated by the tide. In operation, this sheme clearly requires real time measured offshore wave spectra, an option not available to us. This model could be applied to the Strait of Georgia, but only after field studies and the allocation of dedicated wave buoys.

3 APPLICATION TO THE STRAIT OF GEORGIA

Over most of the Strait of Georgia, current shear is not large enough to significantly affect waves and may be ignored to first approximation. Thus the SMB method can be used to forecast values of H_s and T_s without regard for currents. This is done for both Cape Mudge and Sand Heads. Wave current effects are included by: (1) assuming a model spectrum appropriate to H_s and T_s, (2) invoking wave action conservation using predicted currents at Cape Mudge and Sand Heads to derive a modified spectrum, (3) and finally deducing the value of H_s appropriate to the altered spectral distribution. The significant period does not change because the observed frequency is essentially constant. In addition, a new significant wave slope is computed. The ratios of the modified H_s and S_m to their incident values are published as a set of enhancement factors for the possible range of wave periods. Note that the enhancement factors also include shoaling and refractive contributions.

Application of the theory to Cape Mudge and Sand Heads is considered separately because each lies in a distinct oceanographic domain. The procedure is described in detail by example for Cape Mudge, and in so doing, we will also explain how the SMB technique is generalized to temporally varying winds. A few comments specific to Sand Heads close the discussion. The example is repeated in the User's Manual.

3.1 CAPE MUDGE

Application of the SMB method to the Strait of Georgia is greatly simplified by the fact that winds, and especially strong winds, tend to be unidirectional over the Strait - that is they tend to blow up- or down-strait and we assume this to hold exactly here. In addition, we further assume that the winds are of uniform strength over the full fetch, which we estimate to

be 90 km for Cape Mudge and 22 km at Sand Heads (Figure 1). Since the fetch is fixed, duration becomes the sole independent variable in the SMB relations (15)-(17). Traditionally, SMB wave height and period are estimated graphically from a set of curves. We also adopt that procedure but exploit the fixed geometry of the two forecast regions by plotting site specific graphs. This greatly simplifies the charts. In fact, each "graph" is actually composed of a set of two charts. The first member of each pair (Figure 7A) is used as a work sheet over which the second as a transparency is overlaid to read wave period and height. Lines of constant $H_s T_s$, which approximate wave energy in the SMB approach, are plotted on the first sheet, and lines of constant H_s and constant T_s are drawn on the second. When the windspeed changes, the SMB method assumes that the wavefield conserves its energy (*i.e.*, $H_s T_s$ = constant), but that H_s and T_s assume new values appropriate to the new windspeed. In the case of a stiffening wind, this assumption is valid provided that the wind direction does change by more than about 30°. Operationally, this means that the wind does not reverse at Cape Mudge or shift to the SE or NW at Sand Heads. If the wind direction does change, the waves are assumed to be destroyed by the adverse wind, and the wave energy drops to zero over a fairly short period. In the event of a falling wind, the energy level is limited by the saturation energy appropriate to the reduced windspeed. If $H_s T_s$ exceeds the corresponding value for a fully developed sea, H_s and T_s are reduced accordingly.

A history of observed and/or forecast winds is necessary to use the graphs. If forecast winds are provided, the SMB technique obviously works in a forecast mode. Time varying winds are assumed to be piecewise constant and centred on the observation time. Thus for example, if winds are observed every three hours, the wind measured at 0600 PST would be assumed to hold for the period 0430 - 0730 PST. The actual interval is unimportant and the technique can be applied to arbitrary and non-uniform spacing.

Example

The SMB method is now illustrated by example using the hypothetical windfield of June 1, 1987 (Figure 8 and Table 2). Winds are observed every three hours and are assumed constant from the SE over each three hour interval. The sea is assumed calm immediately preceding the event. Consider the first interval which is represented by Point 1 on Figure 7A: windspeed = 4 knots, duration = 3 hours. By overlaying the second sheet on the first, the appropriate wave height and period for hour 4.5 are seen to be approximately 0.25 m and 0.5 s, respectively. Consider now the next interval during which the wind increases slightly to 5 knots. If the sea were initially calm at the start of the interval, we would proceed as before, but it is not. Rather, we calculate the wave energy appropriate to Point 1, and compute new values of H_s and T_s appropriate to the new windspeed by transposing Point 1 parallel to the nearest constant energy curve until the 5 knot level is reached. Thus Point 1 translates along the dotted line to the point indicated by the open square, which represents the initial state for the second three

hour period. At the end of the second interval, the sea state is given by Point 2. The sequence then reiterates. On a falling wind, the procedure is the same except that the constant energy curves are followed "downwards".

The heavy curve on Figure 7 represents a fully developed sea. Once it is reached, wave energy, height, and period remain invariant so long as the wind speed does not change. Its function is illustrated by considering Point 6. To estimate the initial conditions for the following three hour period, the energy curve (horizontal) is traced backwards to the heavy line. Since the subsequent windspeed is smaller, the bold curve is traced downwards to the open square and, the sea remains fully developed but less energetic. (It is implicitly assumed that wave energy is dissipated by whitecapping and by propagation out of the region). If the new windspeed were greater, the appropriate energy curve would be traced back across the heavy line, and the sea would be no longer fully developed.

This concludes the illustration of the SMB method, but it still remains to include wave current interaction. To do so, we assume that the currents are unimportant except in the immediate vicinity of Cape Mudge where they are obtained from the GF7, 2 km grid barotropic tidal model of Crean (1983). In terms of the incident spectrum (denoted by subscript *I*), the modified spectrum (subscript *CM*) is given by

$$E_{CM}(\omega,\theta)=\left(\omega_{oCM}/\omega_{oI}\right)E_I(\omega,\theta) \tag{32}$$

with

$$\omega_{oCM}=\omega_{CM}-\underline{k}\cdot\underline{U}=\omega_I-\underline{k}\cdot\underline{U}, \qquad \omega_{oI}=\omega_I \tag{33}$$

Since the observed frequency ω is constant along a ray, the incident spectrum is defined by (28) with

$$\omega_m=2\pi/T_s \tag{34}$$

and

$$\alpha=\left(\sqrt{5}\pi^2/gT_s^2\right)H_s^2 \tag{35}$$

The method proceeds by first discretising $E(\omega,\theta)$ into a set of frequency and direction bins of width $\Delta\omega = 2\pi/\Delta T$ with $\Delta T = 2$ s and $\Delta\theta = 5$ °. Then (27) is applied to each frequency and relevant direction bin and the result is summed,

$$m_{oCM}=\sum_i\sum_j E\left(\omega_i,\theta_j\right)\Delta\omega\,\Delta\theta \tag{36}$$

By relevant, we refer to those directions which do not correspond to propagation from the boundaries (Figure 9). Finally, a significant wave height enhancement factor R is obtained as the ratio of the modified H_s to its incident value,

$$R=H_{sCM}/H_{sI}=\sqrt{\left(m_{oCM}/m_{oI}\right)} \tag{37}$$

Wave slope is computed in a similar fashion

$$S_m^2 = \sum_i \sum_j k^2(\omega_i) E(\omega_i, \theta_j) \Delta\omega_i \Delta\theta_j \tag{38}$$

where $k(\omega)$ is calculated from the dispersion relation (4) for a water depth of 60 m.

Figure 10 displays the sample results for June 1, 1987. The modified SMB wave heights obtained using the enhancement factors for the case study are listed in Table 2. For a given time, the "HT" enhancement factor (height) corresponding to the predicted significant period ("PEAK PERIOD") is selected and multiplied by the SMB-predicted wave height to give a corrected wave height to be used in forecasts. If the time falls between hours, as it does in this case, the enhancement factor is linearly interpolated between the two published values. Note that because tidal currents vary rapidly in time, the factors do so too (Figure 11). One may also interpolate between peak periods, but the variation with period is much weaker and it is probably sufficient to simply choose the period nearest the predicted one. Recall that the predicted period does not change; it is essentially unaffected by the tidal flow.

Several other parameters are also published in the tables and include the up-strait (v) and cross-strait (u) components of the tidal currents in m/s and the tidal elevation z in m at Cape Mudge. These are not required for the prediction and are included solely for interest, as well as to establish a relationship between tides and waves. The slope enhancement factor "SLOPE" is more important and can be used in precisely the same manner as "HT" to compute a modified mean slope. However, wave slope is not provided by the SMB technique nor is slope often given in an operational wave forecast. It is included here primarily to provide an indication of when seas can be expected to be especially choppy for small boats.

This then illustrates the application of the SMB method and the wave-current modification scheme in practice. Of course it is not necessary to use three hourly winds or to assume that the wind intervals are centred on the observation times. The modifications required to accommodate other choices are obvious.

3.2 SAND HEADS

Sand Heads differs in two important respects from Cape Mudge. The currents capable of modifying waves are largely driven by the Fraser River outflow which is in turn modulated by the tide. Moreover, the Steveston Jetty acts as a barrier to the general NW-SE tidal stream and forces the flow inshore of the jetty to be primarily across-strait. This implies that the important winds are from the SW and not along-strait, since waves and wind are generally aligned and since wave-current interaction is minimal for waves propagating perpendicular to the flow. (On the other hand, the incident wave field "sees" the currents through a $cos^2\theta$ beam, and winds not strictly from the southwest can be significant. Consideration of such cases is important, but it expands a one dimensional problem into two dimensions and thus is not considered further here.)

In contrast to the situation at Cape Mudge, the existing tidal model of the Strait of

Georgia capable of reproducing Sand Heads currents have not yet been run for sufficient periods to permit analysis for tidal harmonic constants. Consequently, we based our current predictions at Sand Heads on measured currents. Two data sets are available: a two month mooring in March - June 1976 and a one month mooring in March - April 1978. The 1976 data are valuable because they span the onset of a strong Fraser River freshet; that is they cover the period when river effects are strongest and when the Coast Pilot warns of adverse sea states. Unfortunately, these data is valid only for speed; measured directions were strongly contaminated by a large iron barge used in the mooring. However, a better mooring was employed in 1978 and both the speed and directional channels were of good quality.

The 1978 data were analysed for the tides and the resulting harmonic constants were used to predict the tidal part of the flow, $\underline{U}_{\mathrm{TIDE}}$. The 1976 data were used to estimate Fraser River effects. Specifically, the daily-averaged outflowing current U was linearly regressed onto the Fraser River daily discharge D metered at Hope. The relation,

$$U = 0.43 + 8.083 \times 10^{-3} D \tag{39}$$

with U in m/s and D in m^3/s accounted for 78% of the current variance and is used to predict U given D. The intercept of 0.43 m/s is close to the value measured in 1978 during low discharge. Thus at any time, the currents at Sand Heads are given by,

$$\underline{U}_{SH} = \underline{U}_{TIDE} + \underline{U}_{FR} \tag{40}$$

with $\underline{U}_{\mathrm{FR}}$ given by (39) and directed parallel to the Steveston Jetty.

Of course, the Fraser River discharge is not known in advance. After discussions with the British Columbia Ministry of the Environment, we elected to use the discharge observed for 1978, since 1978 and 1987 seemed similar in terms of snowpack. This obviously introduces a new source of uncertainty into our estimates. Possible remedies are discussed in Section 4.

4 DISCUSSION AND RECOMMENDATIONS

We have applied a common wave forecasting technique, the SMB method, to the Strait of Georgia and have described a simple modification to include the effects of currents at Cape Mudge and Sand Heads, where wave-current effects are known to be adverse to small boat operators in certain situations. In so doing, a number of significant points have arisen and are discussed here.

First, and of foremost importance, is the need for simultaneous wave and current measurements at these two locations - the model must be validated as well as calibrated. Until it is, the results obtained here are only estimates, albeit conservative ones. In addition, the available current data from Sand Heads are of low quality. The 1976 data, which spans the Fraser River freshet, is accurate only for speed; the compass did not operate properly as the vane was deflected by a large iron platform. The 1978 mooring provided good speed and directional data but only during a period of low run-off.

Second, it is not adequate to assume an idealized Fraser River discharge, since Sand Heads currents are so sensitive to the discharge, and since the discharge can be predicted long in advance with only the same accuracy as the weather. Rather, wave-current predictions should be based on near real time discharge. Hence the full procedure should be automated to run on a computer and should prompt the user for winds and discharge, thus eliminating the need for charts and published enhancement factors. This could be easily accomplished and would require the computing power only of a small PC. In fact we have installed a real time tidal current prediction and drifting object program on a PC for the Environmental Protection Service and the Coast Guard.

Third, current effects are not truly limited to Cape Mudge or Sand Heads, and even if we are interested solely in these locales, spatially varying currents must play some role in modifying the waves along the fetch, especially at Cape Mudge. Wave-current interaction is known to be important in Juan de Fuca Strait (Lambrakos, 1981) and, the model should be extended to the full Fuca-Georgia system.

Fourth, accurate estimation of wave-current effects requires prediction of the directional wave spectrum, a task for which the SMB method was not designed. Its use here was necessitated by the limited nature of this study, but it should be replaced with a more modern technique. Several general options are available and are discussed below. We discount the option of using a better model for m_o alone and assuming a spectral form as unnecessary, given the power of modern microcomputers.

Prior to doing so, however, it is useful to list a set of minimum requirements that we feel are reasonable for any wave model applied to the Georgia-Fuca system. These are:

(1) The model should be compatible with either the GF7 (2 km grid) or GF4 (4 km grid) tidal models of Crean (1983) (Figure 12);

(2) At the very least, it should predict peak period, direction, and some indication of peak shape and directional spread;

(3) It should be readily amended to include wave-current effects.

(4) It should run on an IBM-AT or equivalent system in order that it can easily be installed at the Pacific Weather Centre, and it must be designed to be be user-friendly in the extreme to ensure its use by forecasters.

(5) It should include some measure of non-linear wave-wave interaction;

(6) If the model is extended to the Strait of Juan de Fuca, it should be capable of propagating open ocean swell into the system.

We do not feel it is necessary at this stage to: (1) include shallow water effects (enhanced non-linear interaction and dissipation), or (2) treat the tidal passes connecting Fuca and Georgia (Haro Strait, Boundary Pass) except in a straightforward manner, because the fetch in such regions is very short. However, the model selected should be adaptable to shallow water to accommodate future needs.

4.1 COMPARISON OF AVAILABLE APPROACHES

Three general classes of wave models can achieve all or most of these objectives: coupled hybrid models with parametric and swell modules, decoupled ray models, and fully discrete models. Stronach and Helbig (1986) give a thorough discussion of the strengths and weaknesses of each technique with special emphasis on the inclusion of current effects. Only a few relevant comments are made here.

Before doing so however, it is important to define the difference between windsea and swell. To do so, we must consider the effects of non-linear, wave-wave interaction. The full source term S for the wave energy balance equation can be decomposed into three parts: S_{in} representing energy from the wind, S_{ds} denoting various frictional and dissipative processes, and S_{nl} defining the non-linear, wave-wave transfer of energy. Actually S_{nl} is not a true source term as it describes the conservative transfer of wave energy from one part of $\underline{k}$ - space (or (ω,θ)-space) to another. Physically, non-linear interaction transfers energy from near the peak of the wave spectrum to higher and lower frequencies. Its overriding importance is in determining the shape of the spectrum. Non-linear transfer largely controls the development of a sharply-peaked spectrum and the migration of the peak to lower frequencies as the sea ages, that is as fetch or duration increases.

Windsea refers to that part of the wave spectrum for which non-linear transfer is significant; swell is the low-frequency part of the wave spectrum for which S_{nl} can be neglected in comparison with advection. Slightly below the spectral peak frequency (*i.e.*, at lower frequencies), S_{nl} is very small and the individual wave packets making up the spectrum decouple. They thus propagate along characteristic rays and may gain or lose energy depending on the sum $S_{in} + S_{ds}$. The boundary between swell and windsea is fuzzy and, different workers employ different criteria. One common choice is in terms of the Pierson-Moskowitz peak

frequency ω_{PM} which is the frequency at which the wave phase speed just equals the wind speed and thus at which transfer of momentum and energy from wind to sea must cease. Pierson and Moskowitz (1964) found that

$$\omega_{PM} = (0.13)2\pi g / W_{10} \tag{41}$$

where W_{10} is the windspeed at 10m. Typically, that part of $E(\omega,\theta)$ for which $\omega < (0.8 - 1.0)\omega_{PM}$ is taken as swell.

It is important to appreciate the breadth of this definition: Swell is not limited to waves generated by "distant" storms, rather it applies to any wavefield once the wind dies down. Of course, Juan de Fuca is also subject to swell generated offshore, which must therefore be represented appropriately at the seaward mouth in a wave model. However, no appreciable offshore swell propagates from Fuca into Georgia through the tidal passes.

Wave models are largely defined by their treatment of non-linear interaction. First generation, or completely decoupled, models simply ignore S_{nl} and are thus strictly valid only for swell. They are nonetheless very popular and widely used because they are relatively easy to implement. Second generation models are distinguished by their use of approximations to S_{nl}. In the first of two general classes of second generation models (discrete spectral models) S_{nl} is computed for a family of wave spectra defined in terms of a few parameters and stored in computer memory. Operationally, the model selects the parameterized wave spectrum closest to the computed one at each time step and uses the appropriate stored value of S_{nl}. In the second class of second generation models (parametric models), the problem of computing S_{nl} is avoided by adopting, *a priori*, a specific family of wave spectra. Significantly, both model subclasses use the same parameterized spectrum (JONSWAP spectrum).

We now consider the relative merits of models that could be applied to the Juan de Fuca-Strait of Georgia System.

4.1.1 CHARACTERISTIC MODELS

A characteristic model was used in this application in which discrete, non-interacting wave packets were propagated along ray paths. The simplicity of the characteristic method is very appealing for shallow-water modelling, as only an ordinary differential equation must be solved, and refraction can be included to any desired accuracy. However, the approach suffers two major drawbacks. First, it is impossible to specify S_{nl} along a ray because E must be known for values of ω and θ specific to other rays in the vicinity. This restriction is not overly severe if the transit time of a wave packet from the model boundary to the interior is short compared with the time scale of the non-linear interactions. This time scale may be defined as $E(\omega,\theta)/S_{nl}$ and is typically a few hours. In the present case, the relevant transit time varies with both frequency and location but is generally longer than the non-linear interaction time. This is not to imply that the period of time during which currents significantly modify waves is long, but rather that a wave packet is significantly modified by non-linear transfer during its propagation along a ray. For example, a 4 s wave would require about 8 hours to travel the full

length of the fetch off Cape Mudge. Therefore, it is doubtful that S_{nl} should be ignored in any application to the Fuca-Georgia system.

The second, although less serious drawback to the characteristic approach, occurs for systems in which current refraction is important and the currents are time-dependent, as they are in the present application. Then the rays themselves vary with time and unlike the static case, they must be continuously updated. This is thus a computational and not a theoretical limitation.

4.1.2 PARAMETRIC HYBRID MODELS

The parametric method is based on the experimental finding (K. Hasselmann, *et al.*, 1976) that for most purposes, $E(\omega,\theta)$ can be adequately represented by a few (1-6) time and space varying parameters a_i, i = 1, N. A set of N coupled equations of the form

$$\partial a_i/\partial t + D_{ijk}\partial a_j/\partial x_k + C_{ij}(\underline{a},\underline{u})a_j = S_i(\underline{a},\underline{U},\underline{W}) \quad i = 1,N \tag{42}$$

replaces the wave action balance equation. These equations are solved in finite difference form for the N parameters on a rectangular grid given the overlying windfield and the incident spectrum at any open boundaries. The beauty of the parametric method is that specification of the non-linear transfer becomes very simple: it is implicit in the spectrum itself.

The most sophisticated parametric model (the HYPA model, Gunther and Rosenthal, 1985) has six free parameters and was developed for the North Sea. It uses a parametric directional spectrum of the form

$$E(\omega,\theta) = E_J(\omega)\cos^2(\theta-\theta_o) \tag{43}$$

where $E_J(\omega)$ is the JONSWAP spectrum (K. Hasselmann *et al.*, 1973; Figure 13) defined by:

$$E_J(\omega) = \alpha g^2(2\pi)^{-4}\omega^{-5}\exp\left\{(-5/4)(\omega/\omega_m)^{-4}\right\}\gamma^{\exp\left\{-(\omega/\omega_m-1)/(2\sigma)^2\right\}} \tag{44}$$

Here: α is the Phillips constant and specifies the level of the high frequency tail which asymptotically approaches $\alpha\cdot\omega^{-5}$;

ω_m is the peak frequency, with a lower limit of ω_{PM};

γ is the peak enhancement factor;

$$\sigma = \begin{cases} \sigma_a & \omega < \omega_m \\ \sigma_b & \omega > \omega_m \end{cases}$$

is the left or right peak half width; and

$$\theta_o = arctan\int(\sin\theta E(\omega,\theta)/c_p)d\omega d\theta / \int(\cos\theta E(\omega,\theta)/c_p)d\omega d\theta$$

is the mean windsea propagation direction (based on the wave momentum flux).

For a fully developed sea, $\omega_m = \omega_{PM}$, $\gamma = 1$, and, except for the value of α, $E_J(\omega)$ reduces to the Pierson-Moskowitz fully developed form (28). The three parameters γ, σ_a, σ_b are known as shape parameters as they determine the form of E_J relative to E_{PM}. For a fully developed sea, they have no effect.

For the application of parametric models to Fuca-Georgia, we recommend retention of four parameters, α, ω_m, γ and the wave direction θ_o. The shape parameters would be set equal to their equilibrium values. The physical justification for JONSWAP spectrum-based parametric models lies with the generality with which $E_J(\omega)$ represents observed spectra. Originally derived for growing seas for a fetch limited location off the German coast, $E_J(\omega)$ has been shown to provide a good fit to observed spectra for growing seas away from coastal boundaries (K. Hasselmann *et al.*, 1976).

The representation of the directional part of $E(\omega,\theta)$ is harder to justify. A better choice than the cosine-squared spreading function would be one proportional to $cos^{2p}(\theta-\theta_o)/2$ where p is a frequency dependent coefficient. However, the price paid for such a choice is considerable in terms of computational complexity and, besides, the value of p is not well known. It might be noted, however, that parameterisations of S_{nl} for this form are now available (S. Hasselmann and K. Hasselmann, 1981).

Parametric models based on the JONSWAP spectrum are necessarily deep water models, as the non-linear transfer integral is a strong function of depth in shallow water. However, Bouws *et al.* (1985) have shown an equally valid representation of observed shallow water spectra is given by the TMA spectrum

$$E_{TMA}(\omega,h) = E_J(\omega)\cdot\Phi_{kh}(\omega_h) \tag{45}$$

where

$$\omega_h = \omega(g/h)^{1/2} \tag{46}$$

is a nondimensionalised frequency that varies with depth. The nondimensional function Φ_k varies between 0 and 1, and for frequencies of interest in Georgia is less than 0.9 only for depths shallower than about 20 m. (This conclusion follows from the inequality: $\Phi_k > 0.9$, for $\omega_h > 1.55$.) Thus to first approximation, a JONSWAP based model is appropriate for a Fuca-Georgia model.

Parametric models are most valid for systems in which S_{nl} plays a continuous and dominant role. This criterion may be violated in two distinct ways. For decaying wind systems, S_{nl} decreases and windsea becomes swell. To account for this, the parametric model for the windsea must be married to either a discrete, or more commonly, a characteristic model for the swell. The difficult problem is to specify the windsea-swell transition, or, in the opposing case, the absorption of swell by windsea. The second violation occurs for wind fields that are so inhomogeneous that the advective part of the spectral transport equation is of similar

size to S_{nl}. In this case, the spectrum cannot relax to its parametric form within a single timestep. This is a particular problem for wind systems in which the wind turns rapidly, *e.g.*, for fronts or hurricanes. On the other hand, discrete models fare no better in this circumstance.

In a hybrid model, the swell-windsea interaction processes are highly idealized. Frequency-direction components of the swell spectrum are treated as completely decoupled wave packets, while the windsea part is totally coupled. The transition from windsea to swell is treated as a simple energy exchange, although not necessarily a conservative one. For example, our model dumps windsea into the swell field whenever the Pierson-Moskowitz frequency jumps to a value greater than ω_m due to a relaxing wind. The peak frequency is immediately readjusted to ω_{PM} and the energy excess to that which the new windsea spectrum can accommodate is deemed to be swell and apportioned to appropriate frequency-direction bins. In the opposite case, when the wind strengthens and ω_m drops, what was formally swell is recoupled through non-linear transfer and absorbed into windsea. Our model assumes that all swell with frequencies exceeding 0.9 ω_m is instantaneously absorbed irrespective of its direction. This is accomplished through a readjustment of f_m keeping α constant on the assumption that the high frequency tail is unaffected.

4.1.3 DISCRETE SPECTRAL MODELS

The discrete spectral approach is based on the wave action equation in advective form:

$$\left\{\partial/\partial t + \left(c_{gi} + U_i\right)\partial/\partial x_i + \dot{k}_i \partial/\partial k_i\right\}\left(E(\underline{k})/\omega_o\right) = S \tag{46}$$

Here k is the wave energy propagation velocity in k-space as given by (23). In this method, the energy spectrum is discretised into a number of frequency-direction or wavenumber-direction bins. Given an initial field and subsequent values on the open boundaries, the discrete spectral transfer equation is then solved on a rectangular grid in finite difference form.

The discrete spectral approach is physically appealing because forcing and interaction processes are included explicitly and the problem of windsea/swell interaction is handled naturally. Given the present state-of-the-art, however, this appeal is largely illusory. Present generation discrete spectral models employ parameterized versions of S_{nl}. Thus the dominant process at windsea frequencies is based on parametric forms of $E(\omega,\theta)$. Hence, one may argue that contemporary discrete spectral models are hybrid ones in disguise (and exploit none of the advantages of parametric models). From a slightly different viewpoint, a spectrum discretised into N frequency and M direction bins has N x M degrees of freedom. By contrast, S_{nl}, based on a parametric approximation to $E(\omega,\theta)$ has only a few (1-6). The large mismatch in degrees of freedom would lead to numerical instabilities if S_{nl} were not modified, in some *ad hoc* manner. That is, the effective number of degrees of freedom of $E(\theta,\omega)$ must be reduced to that of S_{nl}. In those models considered by SWAMP (1985), this was accomplished by artificially constraining $E(\theta,\omega)$ to a predetermined shape at high frequencies.

More importantly, the discrete method imposes severe computational requirements.

Assuming that the grid from Crean (1983) 4 km grid tidal model of Fuca-Georgia is used, with about 1,000 active grid points and, that N and M are about 20 each, the discrete spectral approach uses approximately 20 x 20 x 1,000 = 4 x 10^5 variables. By contrast, a parametric model with 4 parameters would require only 4,000. Admittedly, the swell component in hybrid parametric models would also demand computer storage, but relatively few swell directions would be required due to the tendency of winds to blow up- and down-strait. In addition, the time step used by the discrete spectral method which must satisfy

$$\Delta t \leq \Delta x / \sqrt{2} c_{gmax}$$

must be shorter than that used by a parametric model. In fact, parametric models are efficient enough to be run on an IBM AT microcomputer or equivalent whereas the discrete approach requires the resources of a more powerful computer.

4.1.4 SUMMARY OF APPROACHES

To summarize this section, each approach has its own strengths and weaknesses. The characteristic approach has great attraction for shallow water systems but the inclusion of non-linear interaction is a real problem. Moreover, it is best applied to a set of selected points each of which requires a full set of rays. It is more difficult to obtain even coverage over a large region. The discrete spectral method will probably become the dominant one in time, but is presently limited by inflexible parameterisations of S_{nl}. As well, it imposes unacceptable computer demands in a situation in which the exact shape of E is not really vital. Nor have discrete spectral models yet been extended to include currents - a large part of the exercise. By contrast, parametric models do not suffer from those limitations and have already been adapted to include the effects of currents (Stronach and Helbig, 1986), although some routine programming is still required. Finally, the demands of the swell module, which cripple parametric models in some applications, are not large in this case. Consequently, we recommend that a parametric model be implemented for wave prediction in the Strait of Georgia-Juan de Fuca System. Moreover, in its inialial application to the system, we recommend a model based on the JONSWAP deep-water spectrum.

5 REFERENCES

Bouws E., H. Gunther, W. Rosenthal, and C.L. Vincent, 1985. Similarity of wind wave spectrum in finite depth water, 1, Spectral form. *J. Geophys. Res., 90,* 975-986.

Bretschnider, C.L., 1952. Revised wave forecasting relationships. Proc. 2nd Conf. Coastal Eng., Council wave research, Berkeley, CA, 1-15.

Crean, P.B., 1983. The development of rotating, non-linear numerical models (GF2, GF3) simulating barotropic mixed tides in a complex coastal system located between Vancouver Island and the mainland. Can Tech. Rep. Rep. Hydrogr. Oc. Sci. 31, 65pp.

Department of Fisheries and Oceans, 1979. Sailing Directions, British Columbia Coast (south Portion), Vol. 1, ed. J. Watson. Institute of Ocean Sciences, Sidney, B.C.

de Voogt, W.J.P., G.J. Komen and J. Bruinsma, 1985. The KNMI operation wave prediction model GONO. *Ocean Wave Modelling.* The SWAMP Group. Plenum, 193-200.

Gonzales. F.I., 1984. A case study of wave-current-bathymetry interactions at the Columbia River entrance. *J. Phys. Oceanogr.,14,* 1065-1078.

Guddal, J., 1985. The Norwegian wave model (NOWAMO). *Ocean Wave Modelling.* The SWAMP Group. Plenum, 187-191.

Gunther, H. and W. Rosenthal, 1985. The hybrid parametrical (HYPA) wave model. *Ocean Wave Modelling.* The SWAMP Group. Plenum, 211-214.

Hasselmann, K. *et al.*, 1973. Measurements of wind-wave growth and swell decay during the Joint North Sea Wave Project (JONSWAP). *Dtsch. Hydrogr. Z. Suppl. A, 8(12).*

Hasselmann K., D.B. Ross, P. Muller, W. Sell, 1976. A parametric wave prediction model. *J. Phys. Oceanogr., 6,* 200-228.

Hasselmann, S. and K. Hasselmann, 1985. Computations and parameterizations on the non-linear energy transfer i a gravity-wave spectrum. Part I. A new method for efficient computations of the exact non-linear transfer integral. *J. Phys. Oceanogr., 15,* 1378-1391.

Kinsman, B., 1965. *Wind Waves.* Prentice-Hall.

Lambrakos, K.F., 1981. Wave-current interaction effects on water velocity and surface wave spectra. *J. Geophys. Res.,86,* 10995-10960.

LeBlond, P.H., 1981. On the forecasting of extreme sea states. Mar. Environ. Data Serv. Contract. Rep. Ser. *2,* 46 pp.

Longuet-Higgins, M.S. and R.W. Stewart., 1964. Radiation stress in water waves; a physical discussion with applications. *Deep-Sea Research, 11,* 529-562.

Pierson, W.J. and L. Moskowitz, 1964. A proposed spectral form for fully developed wind seas based on the similarity theory of S.A. Kitaigorodskii. *J. Geophys. Res.. 69,* 5181-5190.

Stronach, J.A. and J.A. Helbig, 1986. Numerical prediction of wind-generated waves and wave-current interaction in the coastal waters of northern British Columbia. Institute of Ocean Sciences, Sidney, B.C. 482 pp.

Sverdrup, H.U. and W.H. Munk, 1947. Wind, sea, and swell: theory of relations of forecasting. U.S. Navy Hydrographic Office Pub. No. 601. 44pp.

SWAMP, 1985. *Ocean Wave Modelling.* The SWAMP Group. Plenum.

U.S. Army Corps of Engineers, 1975 *Shore Protection Manual.* Vol. 1. Washington, D.C.

6 TABLES

TABLE 1. SMB Constants

$a_1 = 0.283$	$a_7 = 6.5882$
$a_2 = 0.0125$	$a_8 = 0.0161$
$a_3 = 0.42$	$a_9 = 0.3692$
$a_4 = 1.20$	$a_{10} = 2.2024$
$a_5 = 0.077$	$a_{11} = 0.8798$

TABLE 2

Hypothetical SMB Forecast for Cape Mudge, June 1, 1987.

Time (PST)	Wind Speed (Knots)	SMB H_s (M)	SMB T_p (S)	HT Ratio	Modified H_s (M)
3	4				
		0.25	0.5	---	0.25
6	5				
		0.30	0.75	---	0.3
9	11				
		0.75	1.7	0.73	0.3
12	20				
		1.5	3.1	.86	1.3
15	28				
		2.3	5.	1.48	3.4
18	26				
		2.25	4.9	1.04	2.3
21	11				
		1.2	2.3	0.51	0.6
24	6				
		1.0	0.9	---	0.9

7 FIGURES

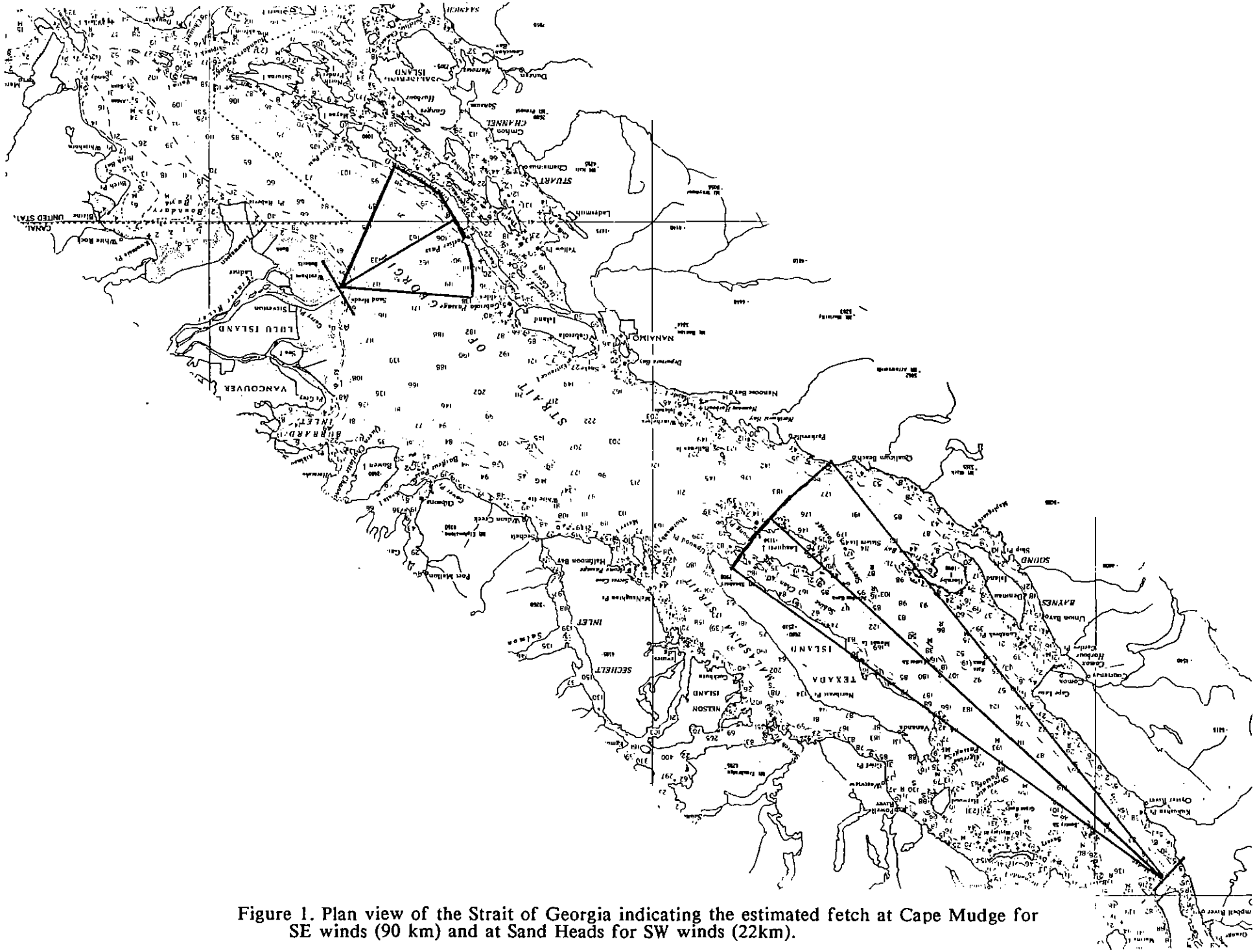

Figure 1. Plan view of the Strait of Georgia indicating the estimated fetch at Cape Mudge for SE winds (90 km) and at Sand Heads for SW winds (22km).

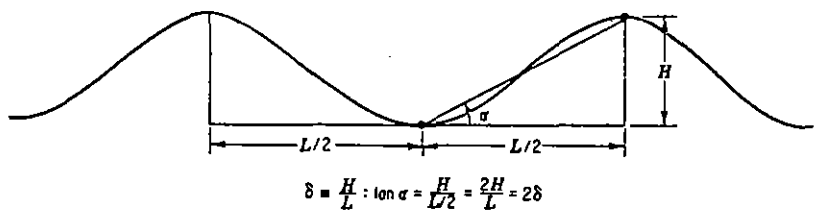

Figure 2A. The geometry of a plane wave illustrating wave height H, wave length L, and mean wave slope α .

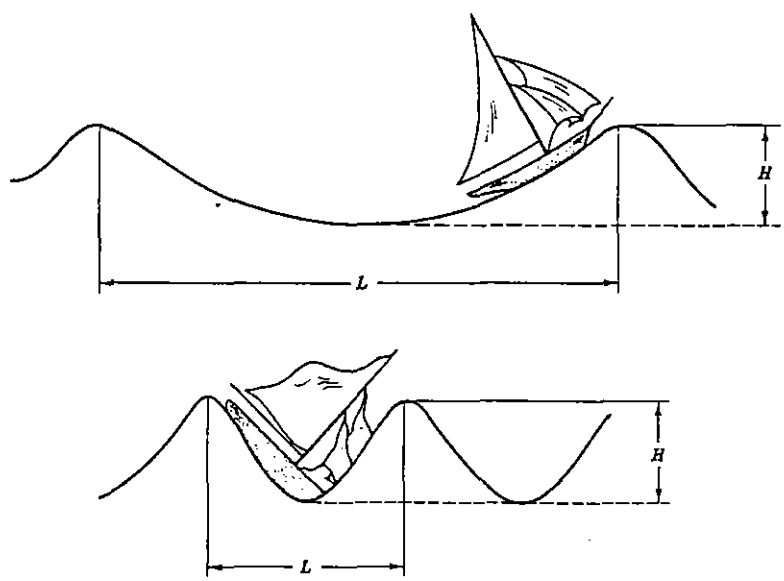

Figure 2B. A schematic illustration of the importance of wave slope.

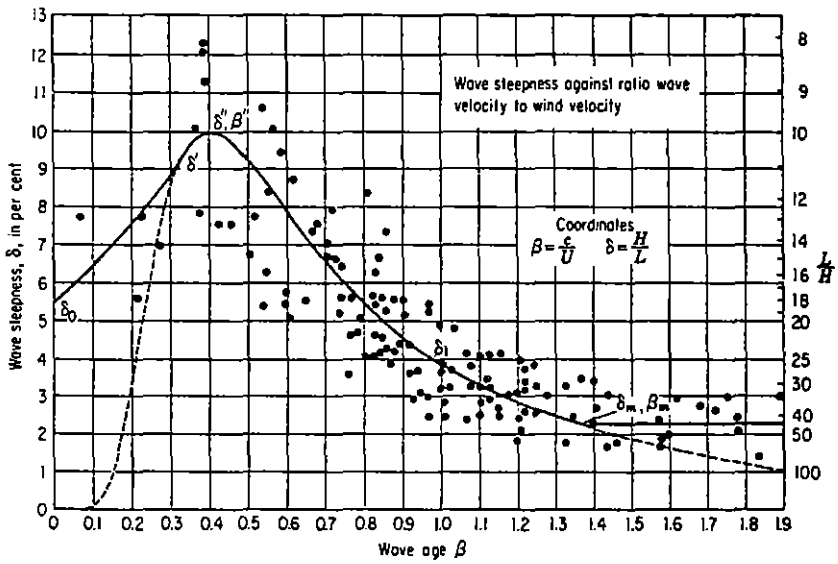

Figure 3. Wave steepness δ as a function of wave age β (from Kinsman, 1965).

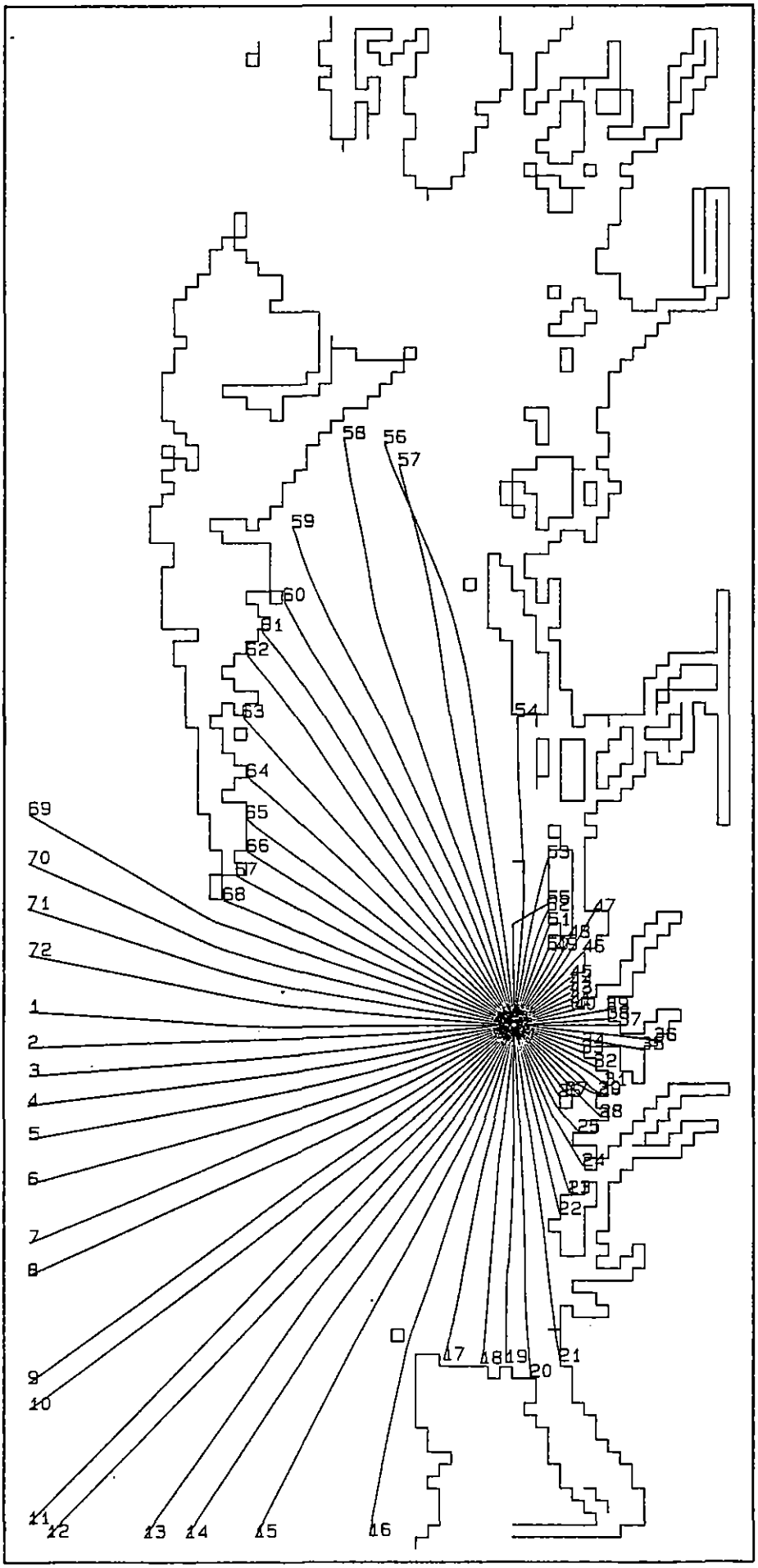

Figure 4. A schematic illustration of the ray backtracing proceedure for a location in Queen Charlotte Sound (from Stronach and Helbig, 1986)

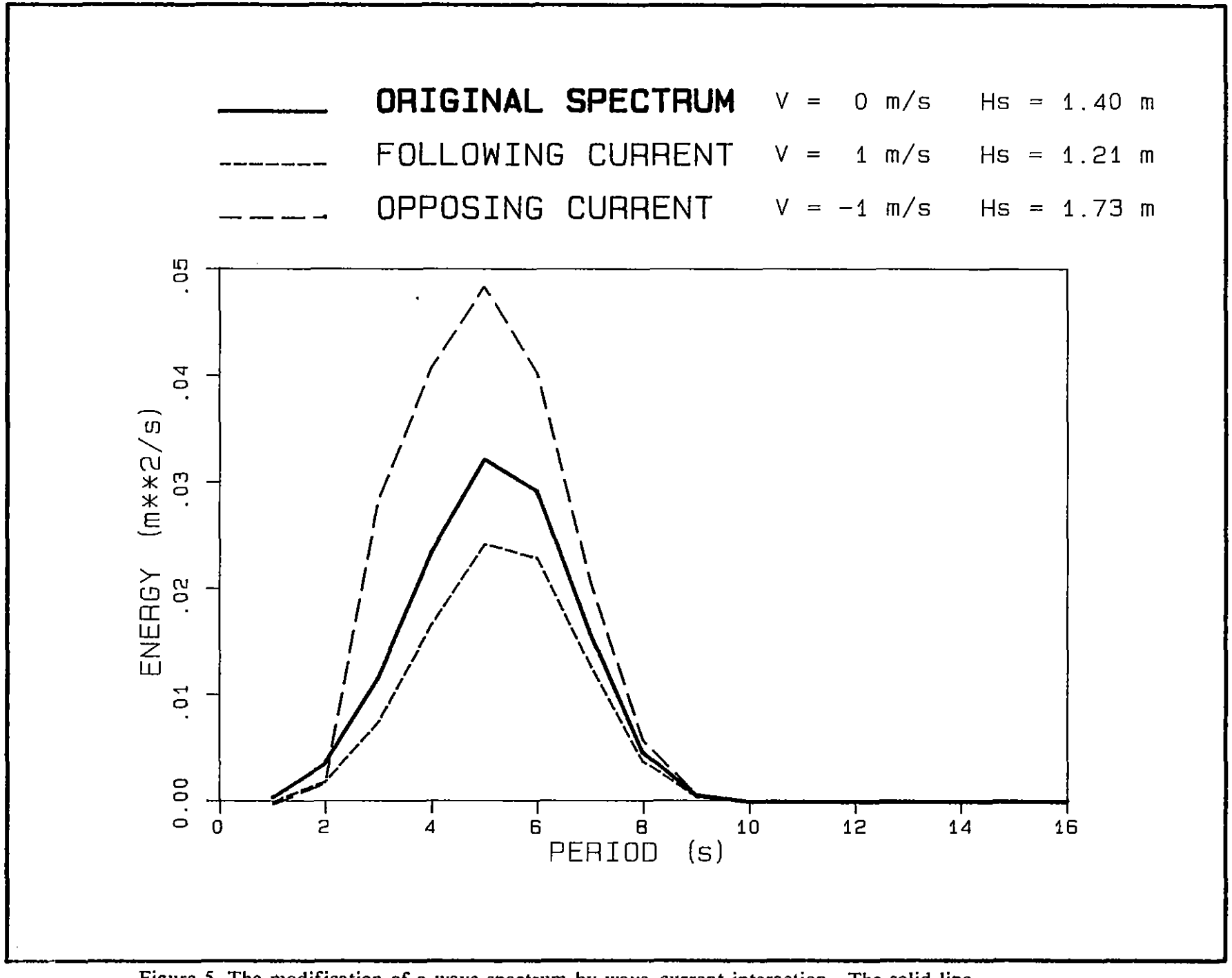

Figure 5. The modification of a wave spectrum by wave-current interaction. The solid line represents the incident spectrum (H_s = 1.4 m); the line of short dashes represents the spectrum when waves propagate with a following current of 1 m/s (H_s = 1.21 m), and the line of longer dashes represents the spectrum when waves propagate into an opposing

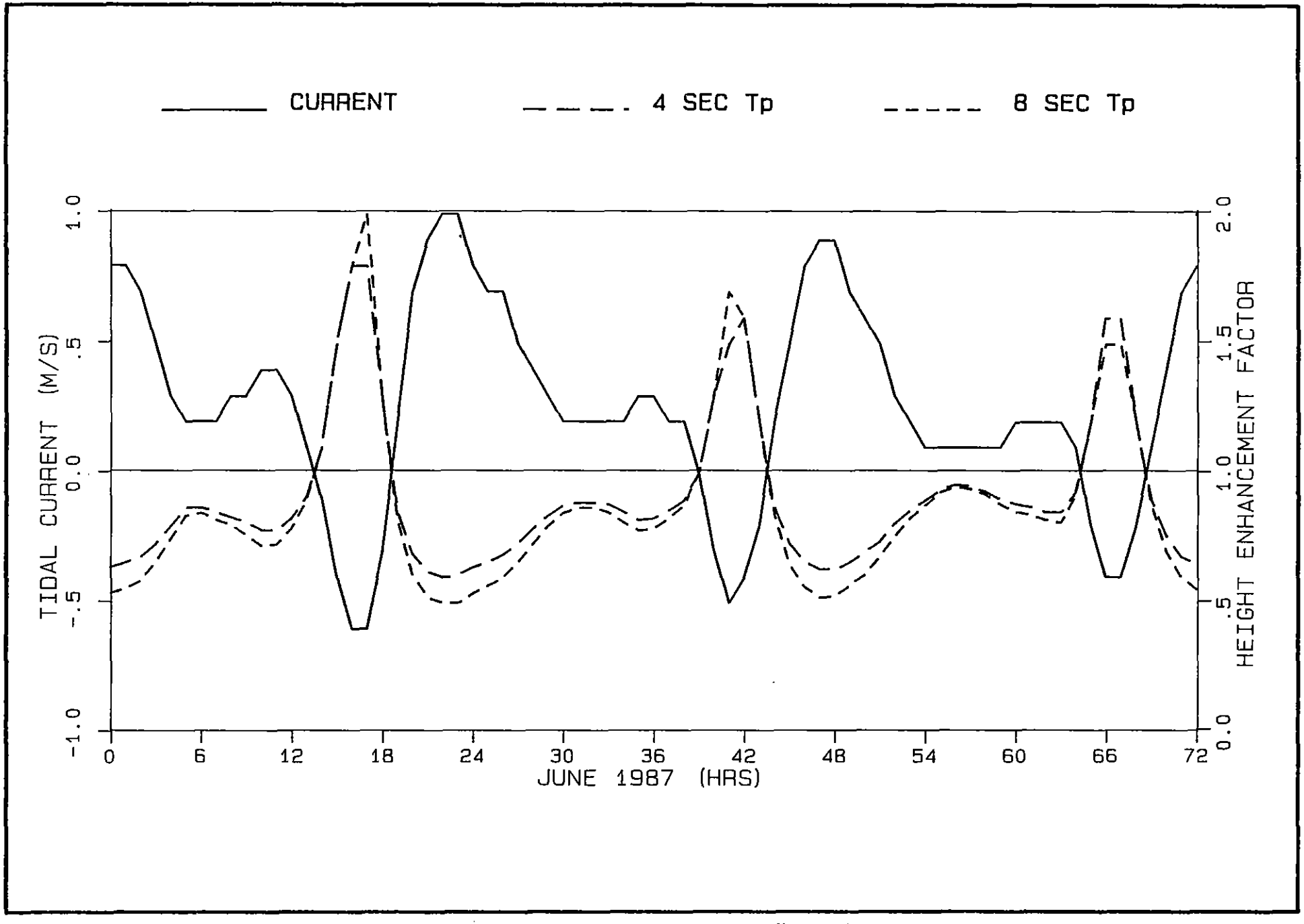

Figure 6. Time series of height enhancement factors for Cape Mudge. The first 72 hours of June 1987 are shown, for waves of peak period 4 s (long dashes) and 8 s (short dashes).

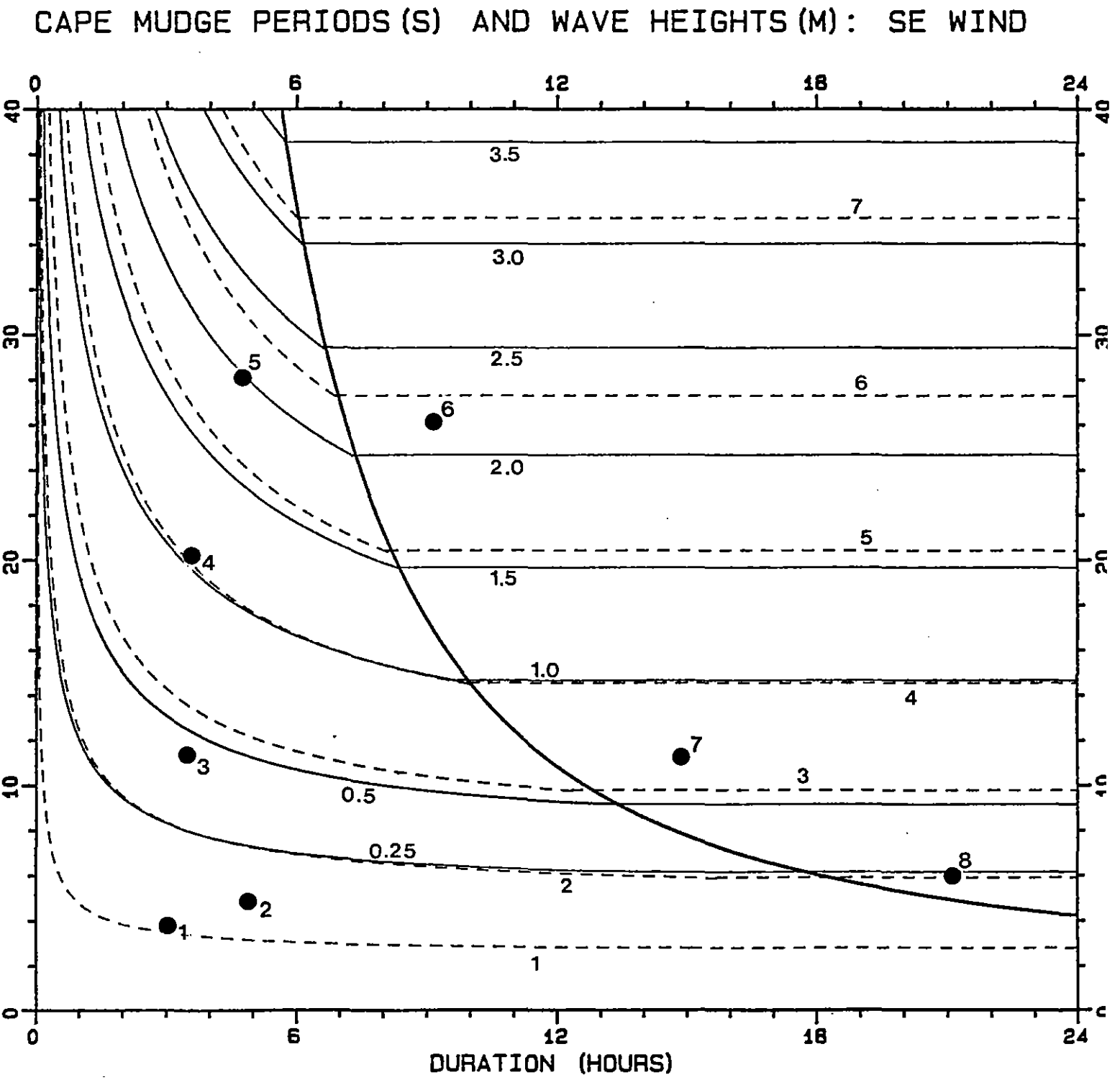

Figure 7A. Forecasting chart 1 for Cape Mudge.

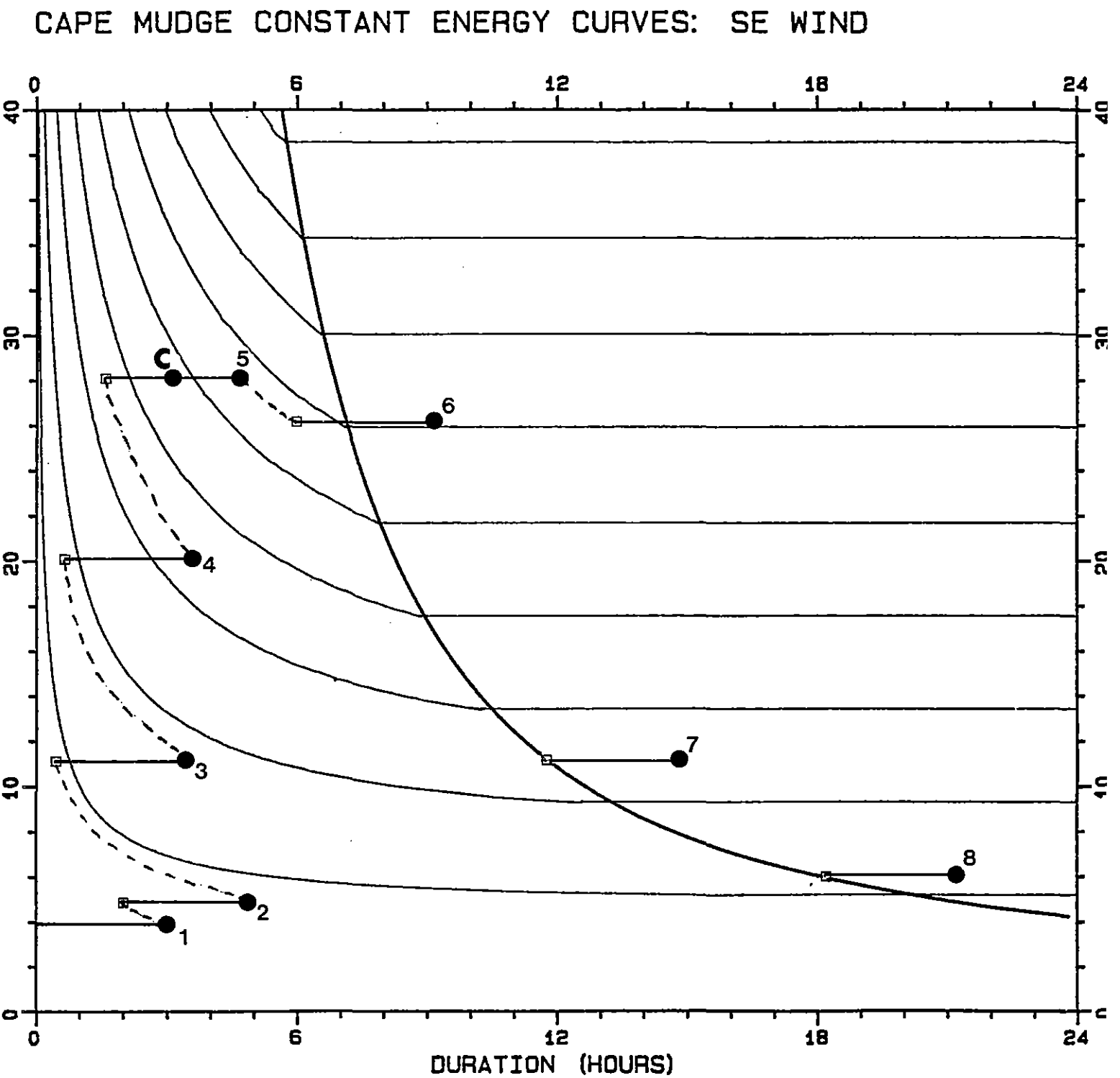

Figure 7B. Forecasting chart 2 for Cape Mudge. Wave heights (solid lines) are given in metres; wave periods (dashed lines) are given in seconds. The area to the right of the heavy solid line represents a fully developed sea.

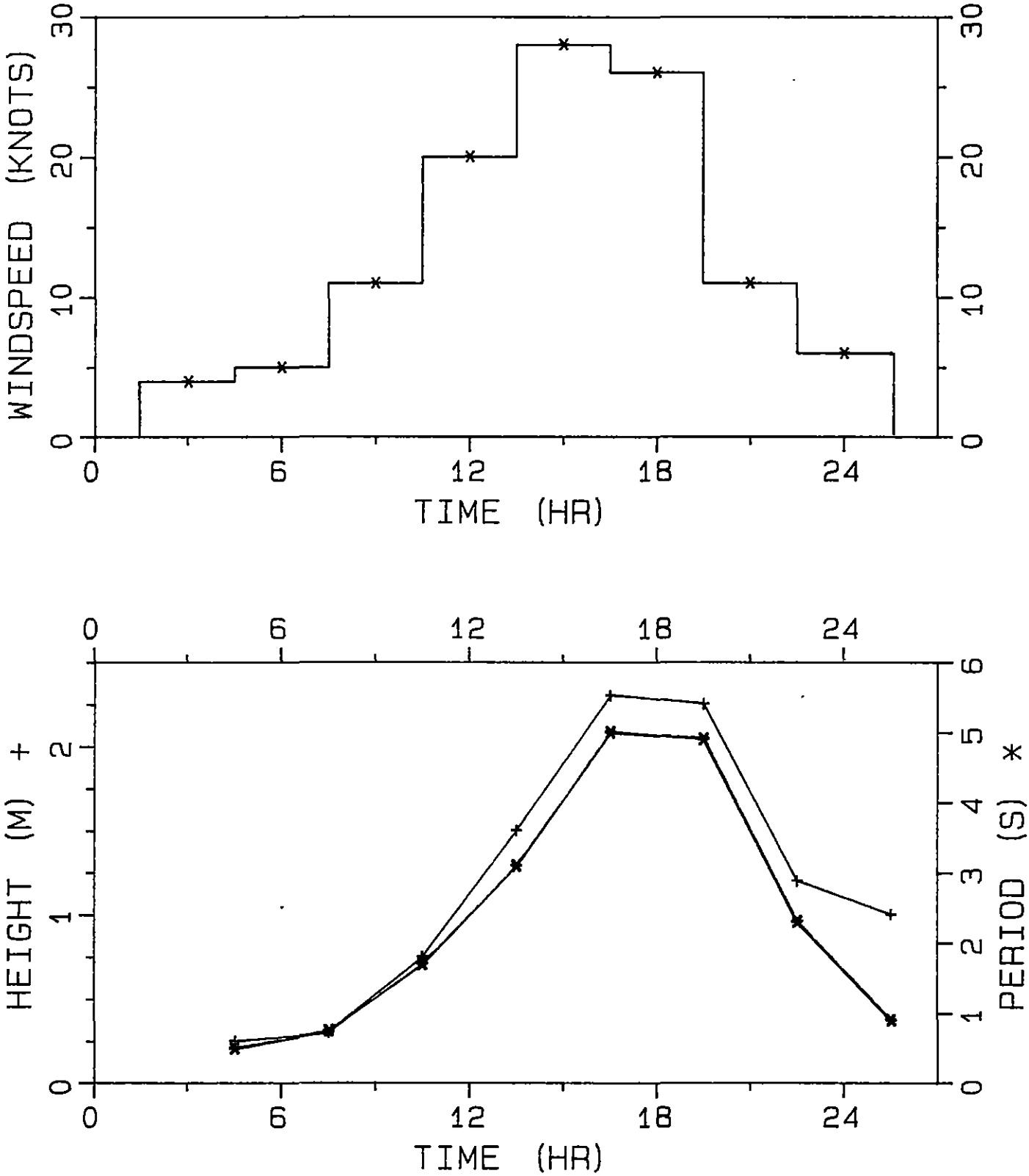

Figure 8. Hypothetical Cape Mudge windfield for June 1, 1987 and SMB predicted wave height and period.

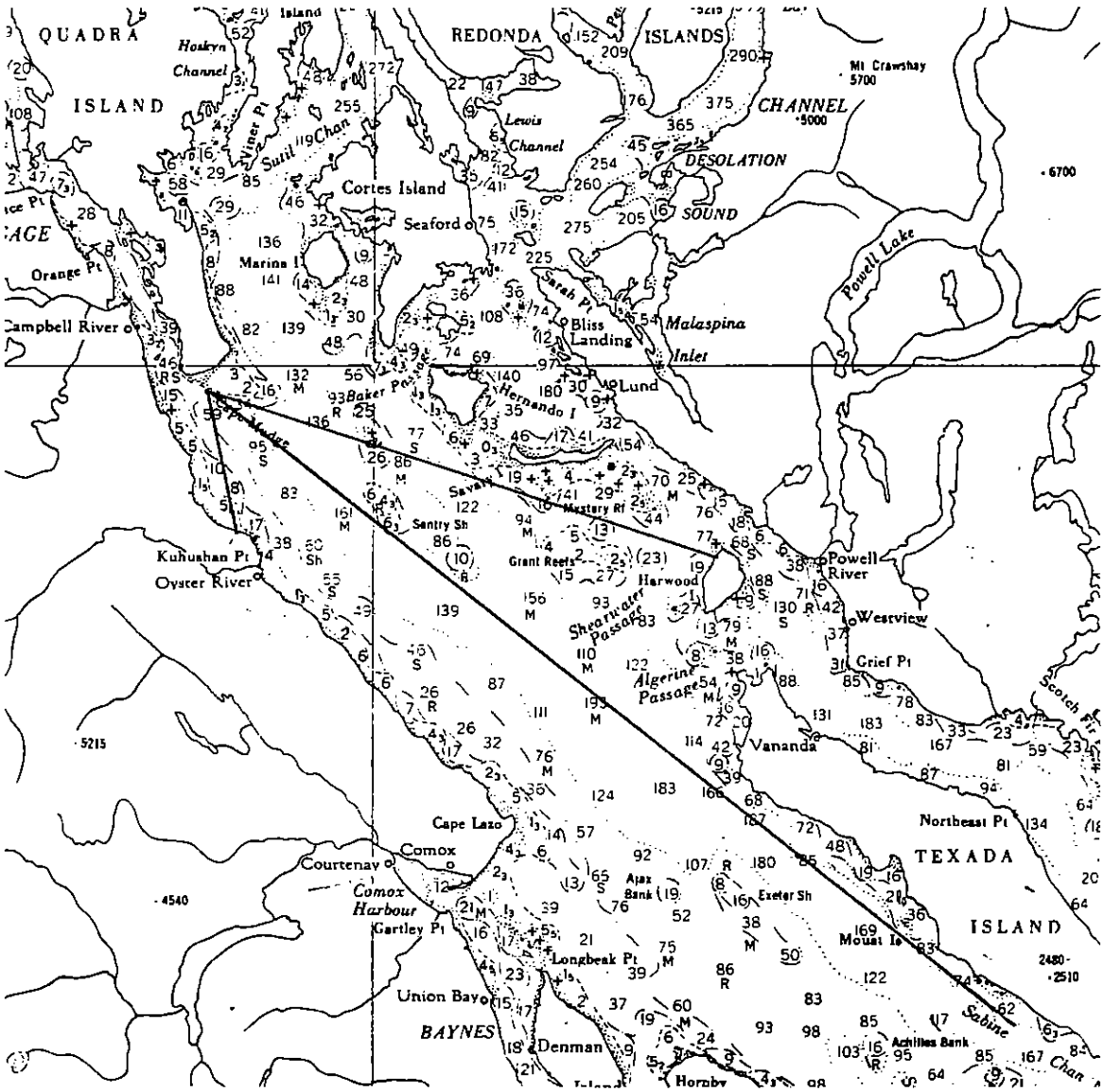

Figure 9. The range of relevant ray directions for Cape Mudge.

CURRENT AND SHOALING ENHANCEMENTS FOR CAPE MUDGE
MONTH: JUNE YEAR: 1987

DAY	HR	U	V	Z	PEAK PERIODS 2.0		3.0		4.0		5.0		6.0		7.0		8.0	
					HT	SLOPE	HT	SLOPE	HT	SLOPE	HT	SLOPE	HT	SLOPE	HT	SLOPE	HT	SLOPE
1	0	-0.3	0.9	4.1	0.52	0.50	0.59	0.51	0.65	0.49	0.70	0.47	0.74	0.47	0.77	0.46	0.79	0.46
1	1	-0.3	0.8	3.9	0.55	0.53	0.62	0.54	0.68	0.53	0.73	0.51	0.76	0.51	0.79	0.50	0.81	0.50
1	2	-0.2	0.8	3.7	0.56	0.55	0.63	0.56	0.69	0.54	0.74	0.53	0.77	0.52	0.80	0.52	0.82	0.52
1	3	-0.2	0.7	3.6	0.59	0.58	0.65	0.59	0.71	0.57	0.76	0.56	0.79	0.56	0.82	0.55	0.84	0.55
1	4	-0.2	0.5	3.6	0.65	0.64	0.71	0.65	0.76	0.64	0.80	0.63	0.83	0.63	0.85	0.63	0.87	0.63
1	5	-0.1	0.3	3.7	0.74	0.74	0.79	0.75	0.83	0.74	0.86	0.74	0.88	0.74	0.90	0.73	0.91	0.73
1	6	-0.1	0.2	3.7	0.82	0.82	0.86	0.83	0.89	0.83	0.91	0.83	0.92	0.82	0.93	0.82	0.94	0.82
1	7	-0.1	0.2	3.7	0.83	0.83	0.86	0.84	0.89	0.84	0.91	0.84	0.93	0.83	0.94	0.83	0.95	0.83
1	8	-0.1	0.2	3.6	0.80	0.80	0.84	0.81	0.87	0.81	0.90	0.80	0.91	0.80	0.93	0.80	0.93	0.80
1	9	-0.1	0.3	3.3	0.78	0.78	0.82	0.79	0.86	0.79	0.88	0.78	0.90	0.78	0.92	0.78	0.93	0.78
1	10	-0.1	0.3	2.8	0.75	0.75	0.79	0.76	0.84	0.75	0.87	0.75	0.89	0.75	0.90	0.74	0.91	0.74
1	11	-0.1	0.4	2.3	0.71	0.71	0.76	0.72	0.81	0.71	0.84	0.70	0.87	0.70	0.88	0.70	0.90	0.70
1	12	0.0	0.4	1.8	0.71	0.71	0.76	0.72	0.81	0.71	0.84	0.70	0.87	0.70	0.88	0.70	0.90	0.70
1	13	0.0	0.3	1.4	0.76	0.76	0.81	0.78	0.85	0.77	0.88	0.77	0.90	0.76	0.91	0.76	0.92	0.76
1	14	0.1	0.1	1.2	0.87	0.87	0.90	0.88	0.92	0.88	0.94	0.88	0.95	0.88	0.95	0.87	0.96	0.87
1	15	0.1	-0.1	1.2	1.11	1.10	1.08	1.09	1.06	1.09	1.05	1.09	1.04	1.09	1.03	1.09	1.03	1.09
1	16	0.2	-0.4	1.6	2.27	1.66	1.83	1.57	1.52	1.55	1.35	1.55	1.25	1.55	1.20	1.55	1.16	1.55
1	17	0.3	-0.6	2.1	2.67	1.70	2.23	1.72	1.84	1.78	1.60	1.82	1.44	1.84	1.34	1.85	1.28	1.86
1	18	0.2	-0.6	2.7	2.66	2.26	2.20	2.05	1.81	2.00	1.57	2.00	1.42	2.00	1.33	2.00	1.27	2.00
1	19	0.0	-0.3	3.3	1.46	1.37	1.33	1.33	1.23	1.32	1.17	1.32	1.13	1.33	1.11	1.33	1.09	1.33
1	20	-0.2	0.2	3.8	0.81	0.81	0.84	0.82	0.88	0.81	0.90	0.81	0.92	0.81	0.93	0.81	0.94	0.81
1	21	-0.3	0.7	4.2	0.60	0.59	0.66	0.60	0.72	0.59	0.77	0.58	0.80	0.57	0.82	0.57	0.84	0.57
1	22	-0.4	0.9	4.4	0.52	0.50	0.59	0.51	0.66	0.50	0.71	0.48	0.74	0.47	0.77	0.47	0.80	0.47
1	23	-0.4	1.0	4.4	0.50	0.54	0.57	0.51	0.63	0.48	0.69	0.46	0.72	0.45	0.75	0.45	0.78	0.45

Figure 10. Significant wave height and wave slope enhancement factors for June 1, 1987. Time is in PST. Also listed are the up-strait (v) and cross-strait (u) components of the tidal current in m/s and the tidal elevation (z) at Cape Mudge.

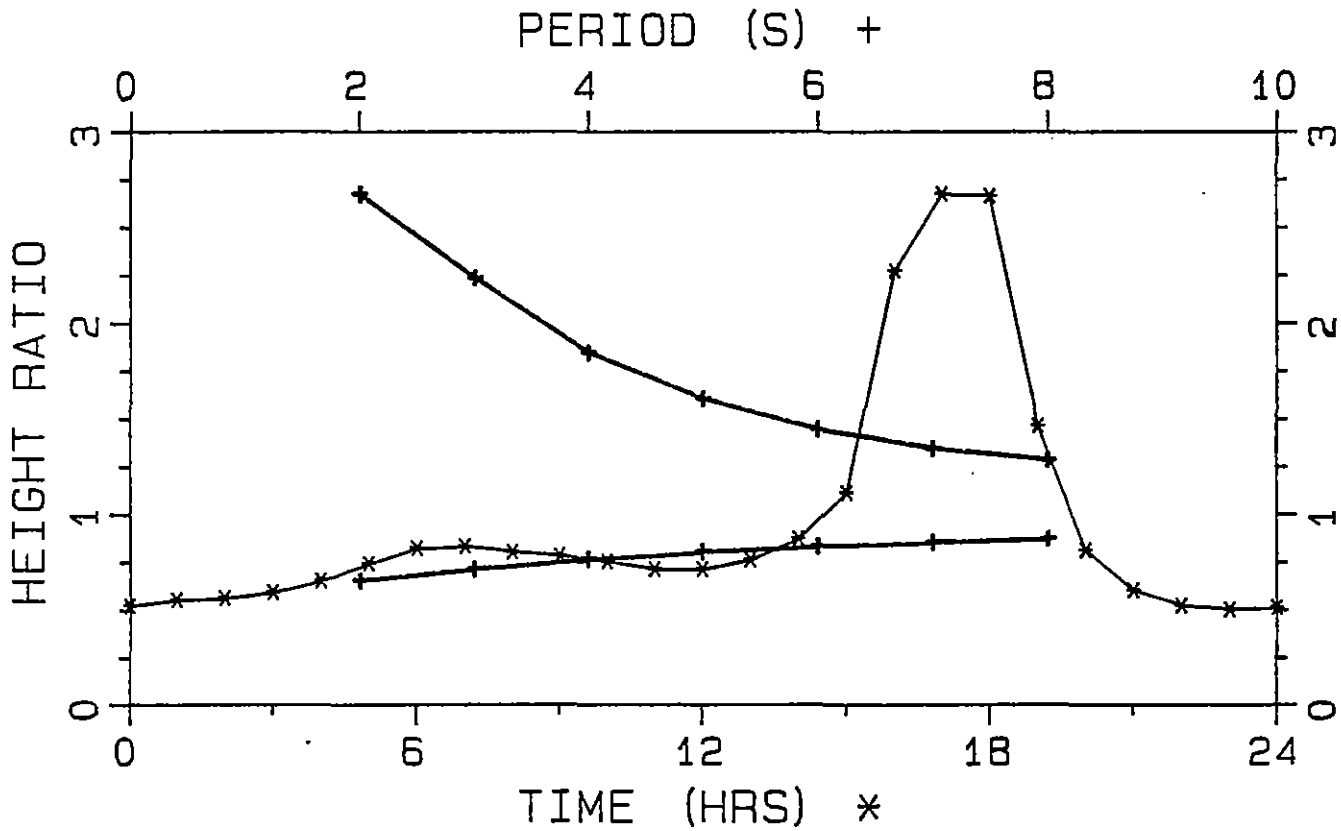

Figure 11. Significant wave height enhancement factors at Cape Mudge for June 1, 1987: (1) vs. time for 2 second waves (*); (2) vs. wave period at 0400 hours (+, lower curve); (3) vs. wave period at 1700 hours (+, upper curve).

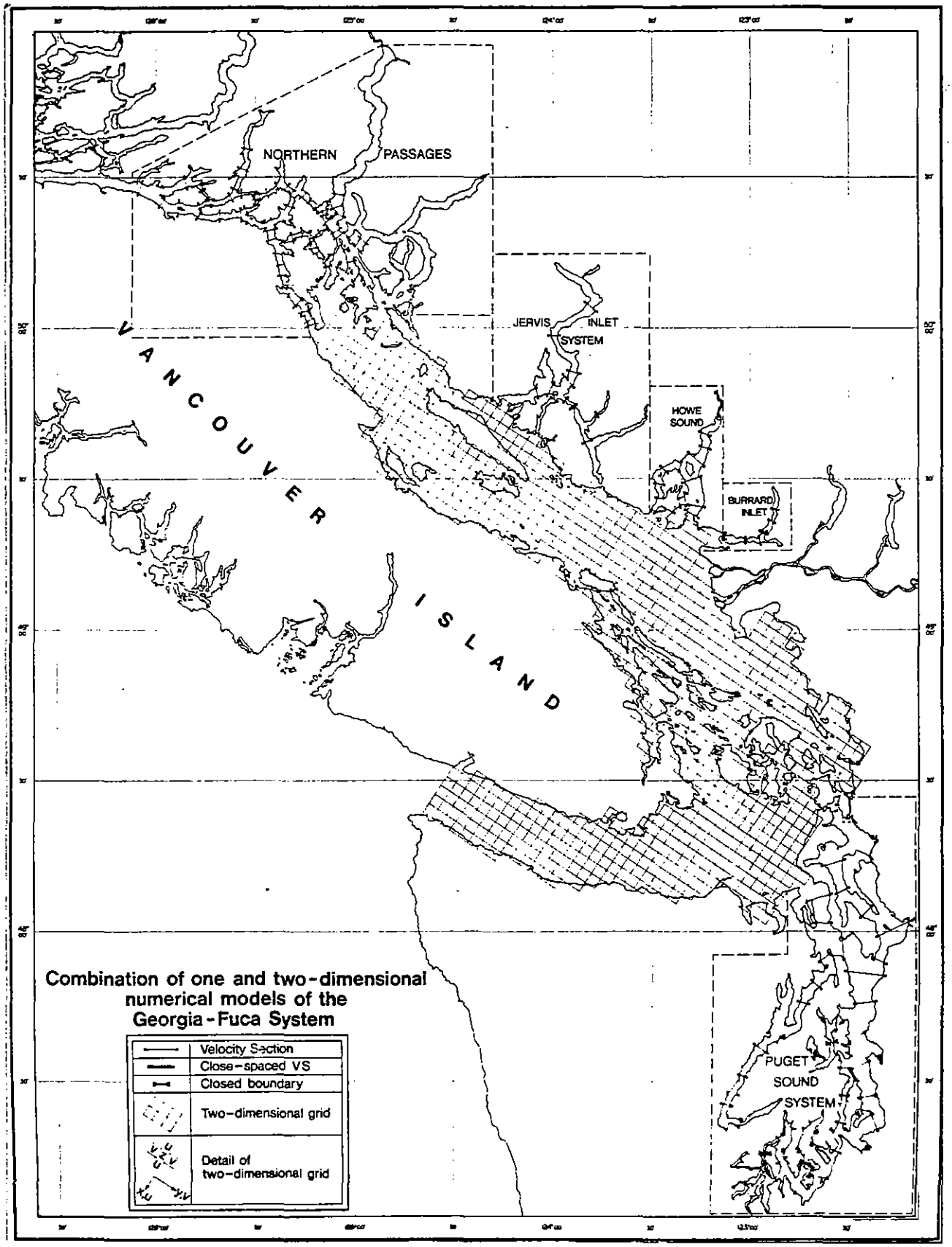

Figure 12. The grid system for the Crean tidal models (from Crean, 1983)

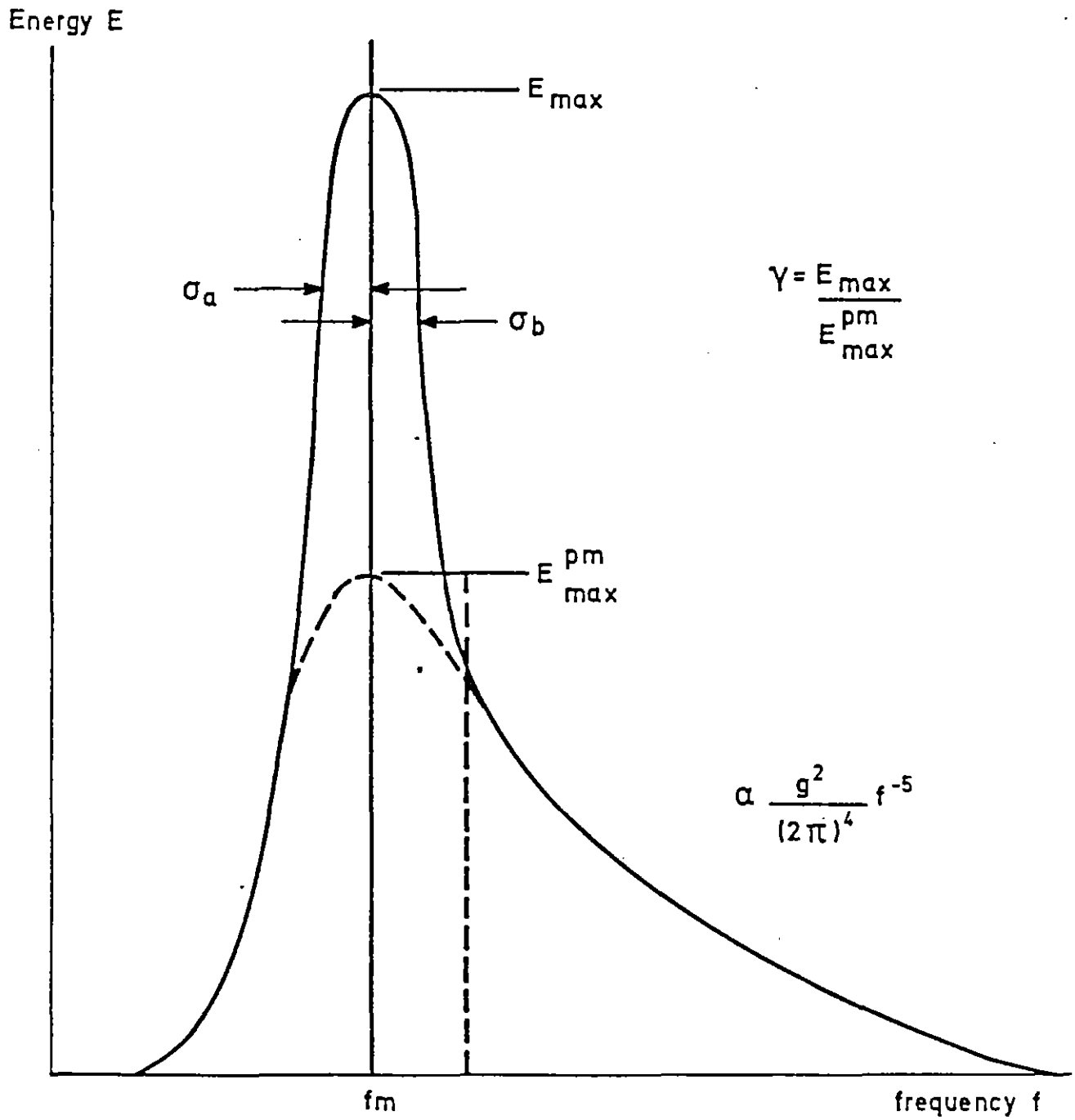

$$E(f) = \alpha g^2 (2\pi)^{-4} f^{-5} \exp\left\{-\frac{5}{4}\left(\frac{f}{f_m}\right)^{-4}\right\} \cdot \ln\gamma \cdot \exp\left[-\frac{(f-f_m)^2}{2\sigma^2 f_m^2}\right]$$

Figure 13. The JONSWAP frequency spectrum.